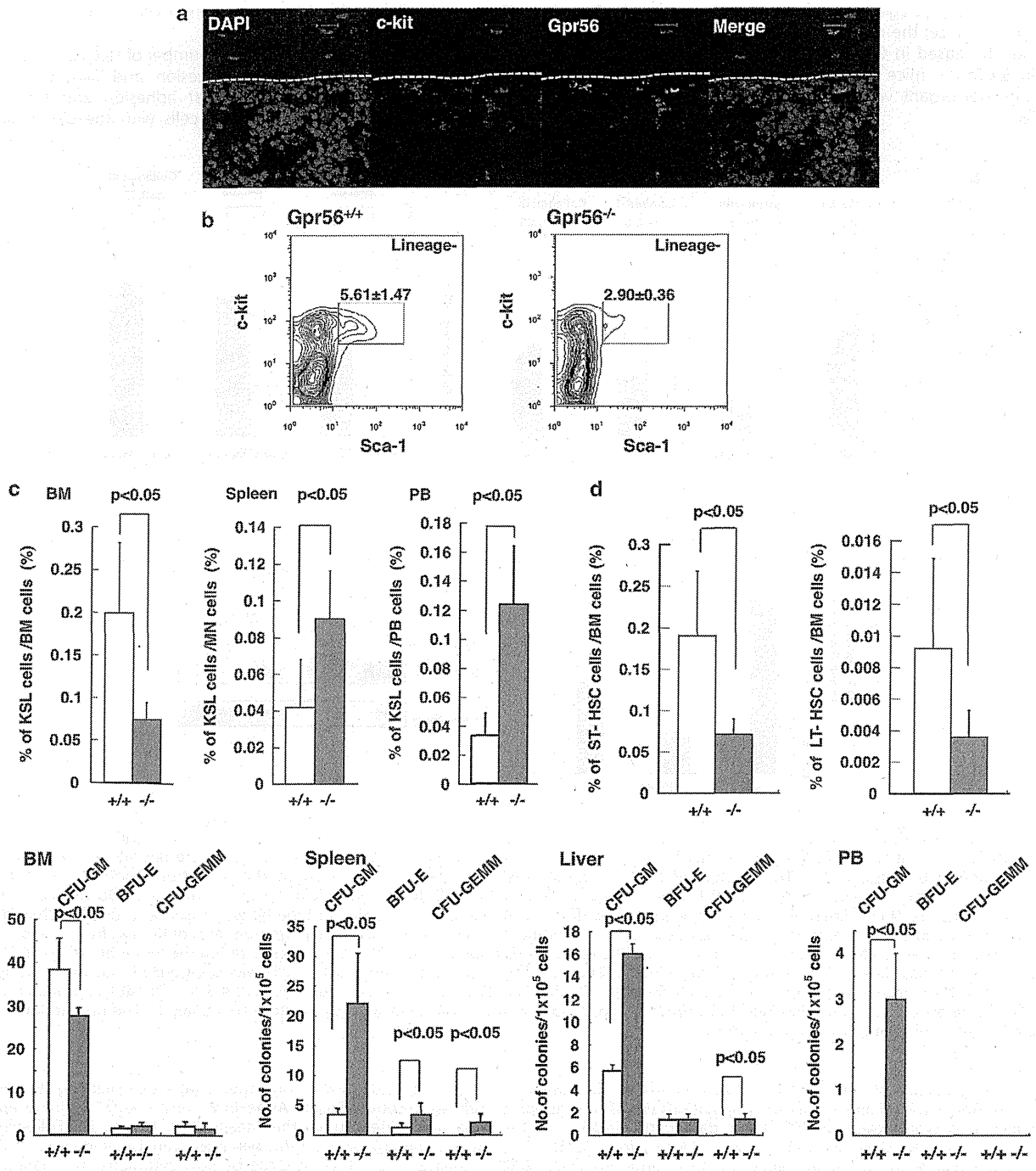


**Figure 6.** Decreased populations of HSCs in the BM of *Gpr56*$^{-/-}$ mice. (**a**) BM sections from wild-type mice were stained with 4′,6-diamidino-2-phenylindole (blue), c-Kit (red) and Gpr56 (white). c-Kit$^{+}$Gpr56$^{+}$ cells resided near the periosteal region in the BM. (**b**) Populations of LSK cells were detected by flow cytometry and were isolated from the BM of 8-to 12-week-old wild-type (*Gpr56*$^{+/+}$) and *Gpr56*$^{-/-}$ mice (*Gpr56*$^{-/-}$). Data are presented as the mean percentages ± s.d. of LSK cells ($n=5$). (**c**) The percentages of LSK cells per total mononuclear cell (MNC) counts in the BM from two legs (left side), the spleen (middle) and the PB (right side) are shown as white bars (+/+) and gray bars (−/−). The proportion of LSK cells in the BM of *Gpr56*$^{-/-}$ mice was significantly decreased, whereas those proportions in the spleen and PB were significantly increased. The data shown are the mean percentages of LSK cells ($n=5$). (**d**) The population of short-term (left side) and long-term (LT) HSCs (right side) are shown as white bars (+/+) and gray bars (−/−). (**e**) The colony-forming abilities of MNCs from the BM, PB, spleens and livers of *Gpr56*$^{+/+}$ (+/+, white bar) and *Gpr56*$^{-/-}$ (−/−, gray bar) mice were determined in methylcellulose cultures by measuring granulocytes/monocytes colony-forming units(CFU-GM), erythroids (burst-forming unit-erythroid, BFU-E) and granulocytes/erythroids/monocytes/megakaryocytes (CFU-GEMM). The data shown are the mean numbers of colonies ($n=3$).

© 2013 Macmillan Publishers Limited

granulocyte/macrophage colony-forming units were maintained in Gpr56$^{-/-}$ mice, the numbers of white blood cells were most likely not decreased in Gpr56$^{-/-}$ mice. Therefore, a part of the HSCs in *Gpr56*$^{-/-}$ mice do not remain in the BM and relocate to the peripheral organs where they maintain their differentiation capacity.

### Decreased cellular adhesion and increased cellular migration ability in HSCs from *Gpr56*$^{-/-}$ mice

To investigate whether the decreased number of HSCs in the BM is related to a reduction in their adhesion and acquisition of migration ability, we assessed cellular adhesion and the cell migration ability using BM precursor cells with the Lin$^-$c-Kit$^+$

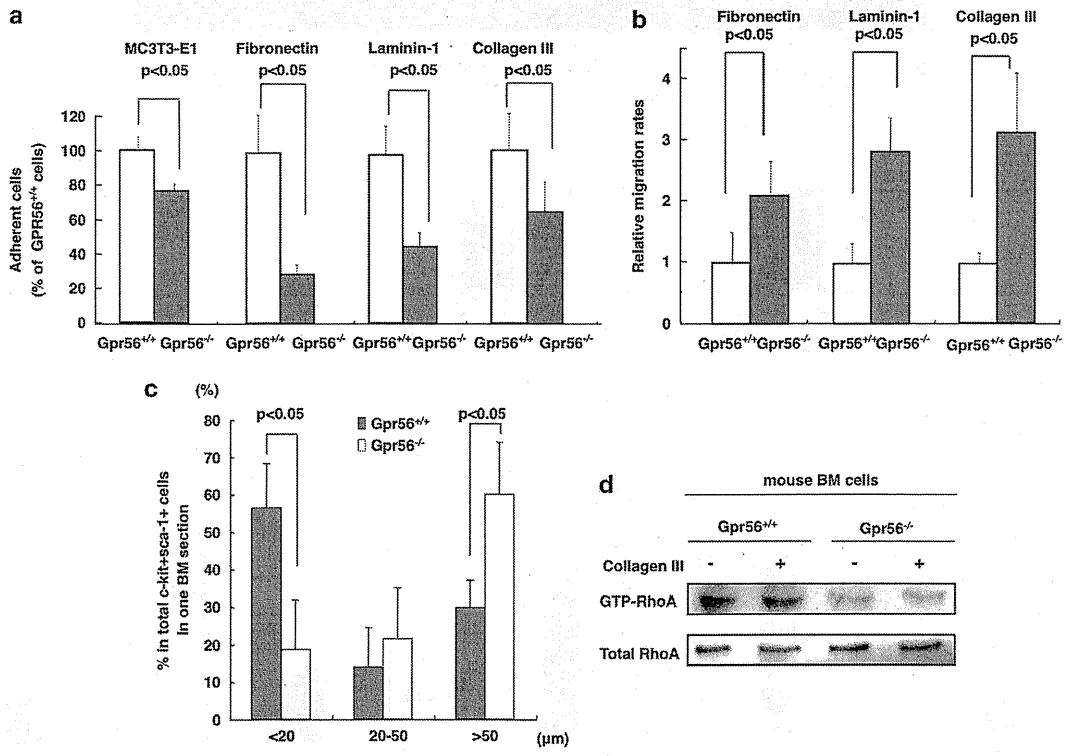


**Figure 7.** Increased migration and decreased cellular adhesion to the ECM of hematopoietic stem/progenitor cells from *Gpr56*$^{-/-}$ mice is induced through the RhoA pathway. (**a**) The adhesion of BM Lin$^-$c-Kit$^+$ (KL) cells from *Gpr56*$^{+/+}$ or *Gpr56*$^{-/-}$ mice to MC3T3-E1 adherent cells and three different types of ECM (fibronectin, laminin-1 or collagen type III) was measured, and the results are displayed as white bars (*Gpr56*$^{+/+}$) or gray bars (*Gpr56*$^{-/-}$). The strength of cellular adhesion is shown relative to the strength of KL cells from *Gpr56*$^{+/+}$ mice. The data are presented as the means ± s.d. ($n=3$) (**b**) The cellular migration of BM KL cells from wild-type or *Gpr56*$^{-/-}$ mice in response to an SDF-1α gradient is shown. Three different types of ECM interfaces (fibronectin, laminin-1 or collagen type III) were used in a Boyden chamber system in this experiment. The data are presented as the relative migration rates compared with the migration rates of KL cells from *Gpr56*$^{+/+}$ mice. The data are presented as the means ± s.d. ($n=3$) (**c**) The *in situ* localization of c-Kit$^+$ and Sca-1$^+$ cells within the femur BM of *Gpr56*$^{+/+}$ or *Gpr56*$^{-/-}$ mice was detected by immunohistochemistry. The localization of c-Kit$^+$ and Sca-1$^+$ cells was categorized into three groups based on the distance from the periosteum (<20, 20–50 and >50 μm). The data are presented as the means ± s.d. ($n=3$). (**d**) The protein level of GTP-bound RhoA in Lin$^-$c-Kit$^+$ BM cells from *Gpr56*$^{+/+}$ or *Gpr56*$^{-/-}$ mice was measured by western blot analysis. The protein level of total RhoA in the cell lysates served as a control.

**Figure 8.** The expression of GPR56 in HSCs is involved in the maintenance of quiescence and LT BM reconstitution. (**a**) After collecting LSK cells labeled with Annexin V-PE and 7-AAD, the populations (%) of early apoptotic cells were counted using Annexin V$^+$ and 7-AAD$^-$ staining, and are displayed as white bars (*Gpr56*$^{+/+}$) or dark bars (*Gpr56*$^{-/-}$). The data are presented as the means ± s.d. ($n=3$). (**b**) Following bromodeoxyuridine (BrdU) incorporation *in vivo*, LSK cells from *Gpr56*$^{+/+}$ (white bar) and *Gpr56*$^{-/-}$ (gray bar) mice were isolated and stained with an allophycocyanin (APC)-conjugated anti-BrdU antibody and 7-AAD to analyze the cell cycle stage by flow cytometry. The data are presented as the means ± s.d. ($n=3$). (**c**) After staining LSK cells from *Gpr56*$^{+/+}$ (left) and *Gpr56*$^{-/-}$ mice (right) with Hoechst 33342 and pyronin Y, the populations (%) of LSK cells in the G0-phase of the cell cycle were assessed via flow cytometry. The data are presented as the means ± s.d. ($n=3$). (**d**) *Gpr56*$^{+/+}$ and *Gpr56*$^{-/-}$ mice were administered 5-fluorouracil intraperitoneally once per week for 2 weeks, and the survival of individual mice was monitored daily. The results were analyzed using a log-rank nonparametric test, and the survival rates of *Gpr56*$^{+/+}$ (solid line) and *Gpr56*$^{-/-}$ (dotted line) mice were plotted on a Kaplan–Meier curve ($n=6$). (**e**) For competitive repopulation assays, donor BM cells or LSK cells from CD45.2$^+$ *Gpr56*$^{+/+}$ or *Gpr56*$^{-/-}$ mice were mixed in a 1:1 or 1:50 ratio with CD45.1$^+$ competitor cells and transplanted into lethally irradiated CD45.1$^+$-recipient mice. (**f** and **g**) The chimerism in the first transplantation was measured as the number of white blood cells from the PB (**f**) and as the number of lineage-negative c-Kit-positive cells from the BM (Lin$^-$c-Kit$^+$ BM) (**g**). (**h** and **i**) The chimerism in the second transplantation was measured as the number of white blood cells from the PB (**h**) and as the number of lineage-negative cells from the BM (Lin$^-$c-Kit$^+$ BM) (**i**) The data shown are the mean percentages ± s.d. of donor-derived cells in the PB at 4 weeks after transplantation ($n=5$). The chimerism in Lin$^-$c-Kit$^+$ BM cells was determined by flow cytometry 16 weeks post-transplantation ($n=5$). (**j** and **k**) LSK cells from CD45.2$^+$ wild-type or *Gpr56*$^{-/-}$ mice were used for a competitive repopulation assay. The chimerism in the transplantation was measured as the number of white blood cells from the PB (**j**) and as the number of lineage-negative c-Kit-positive cells from the BM (Lin$^-$c-Kit$^+$ BM) (**k**). The data shown are the mean percentages ± s.d. of donor-derived cells in the PB at 4 weeks after transplantation ($n=4$).


© 2013 Macmillan Publishers Limited

phenotype. The BM precursor cells in *Gpr56*$^{-/-}$ mice displayed decreased adhesion to MC3T3-E1 cells, fibronectin, laminin-1 and collagen type III as extracellular matrices (Figure 7a). The ability of BM precursor cells from *Gpr56*$^{-/-}$ mice to migrate towards the chemoattractant stromal cell-derived factor-1 was significantly increased on the three types of coated extracellular matrices (Figure 7b). In the next experiment, we determined the precise localization of HSCs in the BM using confocal microscopy after staining BM sections with phycoerythrin-conjugated c-kit and fluorescein isothiocyanate-conjugated Sca-1 antibodies. The

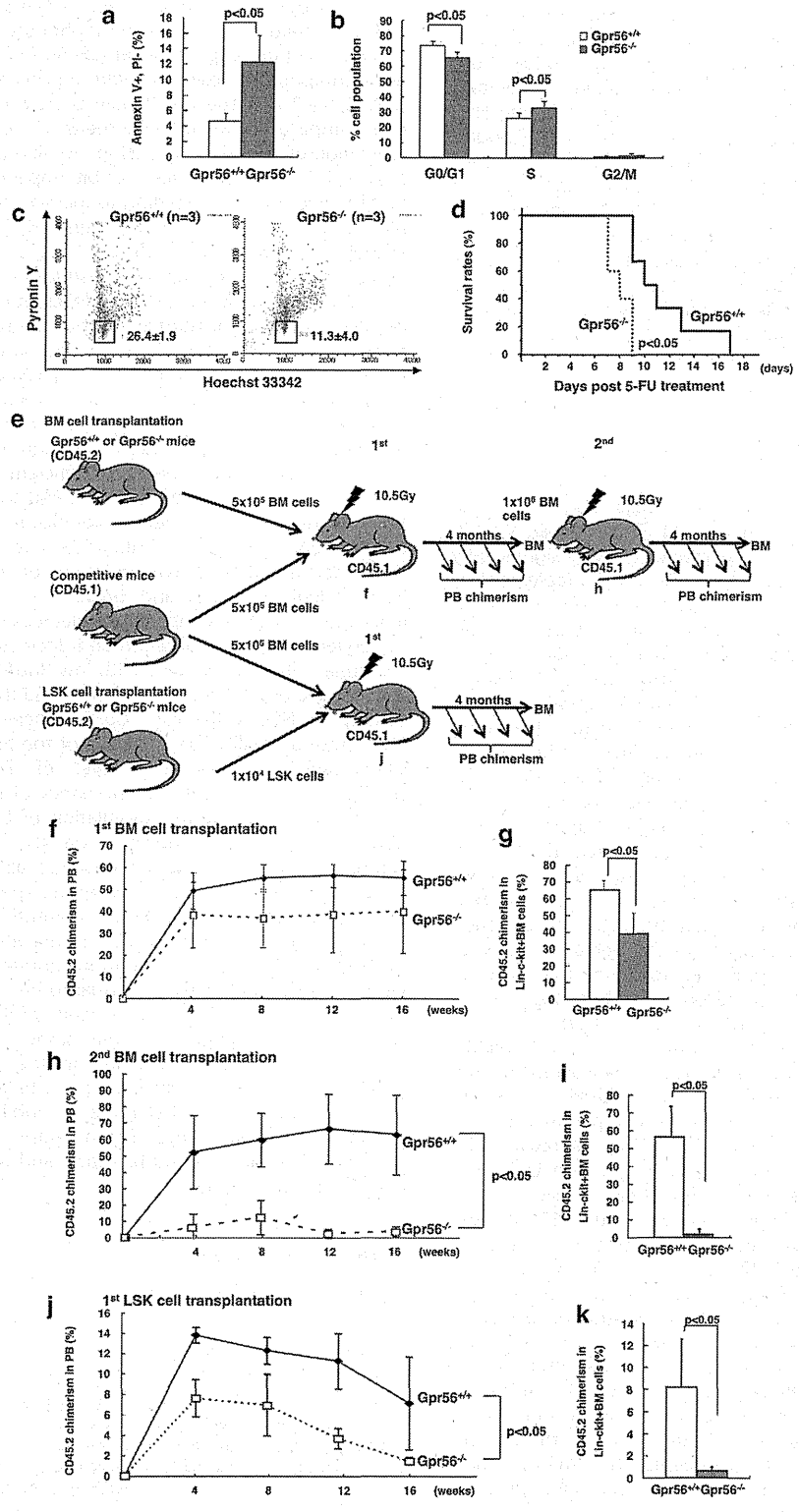


© 2013 Macmillan Publishers Limited

number of primitive cells located less than 20 μm from the periosteum was significantly decreased in the *Gpr56*$^{-/-}$ mice (Figure 7c and Supplementary Figure 10). By contrast, the number of cells that were located more than 50 μm from the periosteum was increased in the *Gpr56*$^{-/-}$ mice. Finally, to investigate whether the migration and adhesion abilities of HSCs depend on GPR56 signaling through the $G\alpha_{12/13}$ and Rho signaling pathway, we determined the protein levels of GTP-bound RhoA in the HSC fractions of wild-type and *Gpr56*$^{-/-}$ mice (Figure 7d). High levels of GTP-bound RhoA accumulated in wild-type mice under both nonstimulated and collagen type III-stimulated conditions, although the stimulation mechanism was unknown in the HSC fraction of wild-type mice. Conversely, low levels of GTP-bound RhoA were detected in the *Gpr56*$^{-/-}$ mice in both the untreated and collagen type III-treated BM cells. In addition, the ability of HSCs to adhere to MC3T3-E1 cells or to fibronectin was significantly decreased by the treatment with Y-27632, a p160ROCK kinase inhibitor (Supplementary Figures 11a and b). Thus, the data suggest that the cellular adhesion of HSCs was decreased by the reduction of RhoA signaling activity, resulting in a reduction in HSCs near the periosteum.

### The expression of GPR56 in HSCs was involved in the maintenance of quiescence and long-term BM reconstitution

Because the fraction of LSK cells in *Gpr56*$^{-/-}$ mice was decreased in the BM along with a reduction in their adhesion ability, we next investigated the fraction of apoptotic cells and cell cycle parameters in the LSK fraction in the BM. The Annexin V$^{+}$7-7-aminoactinomycin D$^{-}$ fraction of apoptotic cells was significantly increased in *Gpr56*$^{-/-}$ mice (Figure 8a and Supplementary Figure 12). The population of G0/G1-phase cells was also decreased, together with an increased population of S-phase cells in the *Gpr56*$^{-/-}$ mice (Figure 8b). Furthermore, the population of G0-phase cells separated by pyronin Y and Hoechst 33342 staining was significantly reduced in the LSK fraction in *Gpr56*$^{-/-}$ mice compared with the population in wild-type mice (Figure 8c). In the next experiment, to determine the drug sensitivity of BM cells in the *Gpr56*$^{-/-}$ mice to an anticancer drug, 5-fluorouracil was injected at a dose of 150 mg/kg once per week for 2 weeks into each of six wild-type and *Gpr56*$^{-/-}$ mice (Figure 8d). The median lifespan of the wild-type mice was 10.5 days, whereas the lifespan of the *Gpr56*$^{-/-}$ mice was significantly shortened to 7.5 days ($P<0.05$); this result suggests that the reduction of the HSC population in the BM and the decreased proportion of G0-phase cells resulted in enhanced cytotoxicity in the *Gpr56*$^{-/-}$ mice in response to this anticancer drug. Finally, to define the ability of HSCs in the *Gpr56*$^{-/-}$ mice to reconstitute hematopoiesis, a mixture of CD45.2$^{+}$ BM cells from wild-type or *Gpr56*$^{-/-}$ mice with CD45.1$^{+}$ competitor BM cells was transplanted into lethally irradiated CD45.1$^{+}$ mice (Figure 8e). In the first transplantation, the population of CD45.2$^{+}$ white blood cells from *Gpr56*$^{-/-}$ mice in the PB was decreased in the recipients compared with the population in the wild-type mice (Figure 8f). Moreover, the population of myeloid, erythroid, megakaryocyte and Lin$^{-}$c-Kit$^{+}$ BM cells from *Gpr56*$^{-/-}$ mice in the recipient BM was significantly decreased (Figure 8g and Supplementary Figure 13). In the second transplantation, the population of white blood cells from *Gpr56*$^{-/-}$ mice was significantly diminished in the PB and Lin$^{-}$c-Kit+ BM cell fractions of the recipients (Figures 8h and i).

Furthermore, to confirm the reduced reconstitution ability of the stem cell fraction in the *Gpr56*$^{-/-}$ mice, we transplanted $1 \times 10^{4}$ LSK cells from wild-type or *Gpr56*$^{-/-}$ mice with CD45.1$^{+}$ competitor BM cells into lethally irradiated CD45.1$^{+}$ mice. As shown in Figures 8j and k, the population of white blood cells from *Gpr56*$^{-/-}$ mice was significantly decreased in the PB and Lin$^{-}$c-Kit+ BM cell fractions of the recipients. Thus, the reduction of cell numbers and the depletion of the quiescent cell population in BM-derived HSCs may result in a reduced capacity for HSC reconstitution in *Gpr56*$^{-/-}$ mice.

## DISCUSSION

In this study, RhoA signaling through $G\alpha_{12/13}$ coupled with GPR56 is a novel signaling pathway for HSC maintenance in BM, which is regulated by EVI1. As high levels of GPR56 expression correlate with the cellular transformation phenotypes of several cancer tissues,[21–23] high expression of GPR56 in EVI1$^{high}$ AML cells may result in apoptotic resistance with a poor prognosis.

Rac1/Rac2 and the Rho family GTPase Cdc42 previously have been implicated in the maintenance of HSCs through the regulation of adhesion, migration, homing and mobilization. HSCs from Cdc42-deficient mice exhibit impaired adhesion, homing, lodging and retention, leading to massive cellular egress from the BM to distal organs and PB, ultimately resulting in failure of engraftment.[25,29] Rac-1-deficient HSCs show a significant reduction in hematopoietic reconstitution, without any effect on cellular adhesion. However, Rac2-deficient HSCs exhibit decreased cellular adhesion but normal short-term engraftment, suggesting a prominent role for Rac2 in integrin-mediated stem cell adhesion.[26–28] On the other hand, P190-B RhoGAP is a major regulator of Rho GTPases, and abnormally high levels of active RhoA protein were detected in embryo-derived cells from P190-B-deficient mice. The migration and adhesion of hematopoietic progenitor cells from the P190-deficient mice were markedly enhanced in an *in vitro* experiment, and the high levels of active RhoA were associated with a significant enhancement of HSC engraftment and reconstitution *in vivo*.[32] In this study, we demonstrated that downregulation of GPR56 expression in EVI1$^{high}$ leukemia cells and *Gpr56*$^{-/-}$ LSK cells caused RhoA inactivation with a concomitant decrease in cellular adhesion. Moreover, apoptotic cell death and decreased G0 cell fractions in leukemia cells and HSC cells with low RhoA activity were found in both *in vitro* and *in vivo* experiments, and the inactivation of RhoA activity in HSC cells from *Gpr56*-deficient mice reduced the reconstitution ability. On the basis of the findings of P190-B- and GPR56-deficient mice, the level of RhoA activation may significantly influence the maintenance of the HSCs in BM.

Rac is activated by the stimulation of CXCR4 by stromal cell-derived factor-1, by adhesion via β1 integrin, and by the stimulation of c-Kit by stem cell factors, all of which are involved in stem cell engraftment. However, no specific ligands of GPR56 other than collagen type III are currently known. Because the expression level of GPR56 was significantly higher in CD34$^{+}$ CD38$^{-}$EVI1$^{high}$ LSC fractions than in normal HSCs (Supplementary Figure 14), GPR56 has the potential to become a novel molecular target in EVI1$^{high}$ leukemia. The results of this study have led to a significant improvement in our understanding of stem cell retention in BM and trafficking in the peripheral circulation. Furthermore, if the specific ligand of GPR56 is identified, we will be able to develop a small-molecule inhibitor or antibody as a specific therapeutic target for refractory leukemia that could modulate the adhesion, mobilization and proliferation abilities of EVI1$^{high}$ leukemia cells.

## CONFLICT OF INTEREST

The authors declare no conflict of interest.

## ACKNOWLEDGEMENTS

We gratefully acknowledge Genentech for providing the *Gpr56* knockout mice for the studies. This work was supported by a grant-in-aid for the third term comprehensive 10-year strategy for cancer control from the Ministry of Health and Welfare; a grant-in-aid for scientific research from The Ministry of Education, Culture, Sports, Science and Technology; a grant-in-aid for scientific research from the Japan Society for the Promotion of Science; and a Grant-in-Aid for Scientific Research on Innovative Areas.


© 2013 Macmillan Publishers Limited

## REFERENCES


1 Ishikawa F, Yoshida S, Saito Y, Hijikata A, Kitamura H, Tanaka S *et al.* Chemotherapy-resistant human AML stem cells home to and engraft within the bone-marrow endosteal region. *Nat Biotechnol* 2007; **25**: 1315–1321.
2 Lane SW, Scadden DT, Gilliland DG. The leukemic stem cell niche: current concepts and therapeutic opportunities. *Blood* 2009; **114**: 1150–1157.
3 Morishita K, Parker DS, Mucenski ML, Jenkins NA, Copeland NG, Ihle JN. Retroviral activation of a novel gene encoding a zinc finger protein in IL-3-dependent myeloid leukemia cell lines. *Cell* 1988; **54**: 831–840.
4 Morishita K, Parganas E, William CL, Whittaker MH, Drabkin H, Oval J *et al.* Activation of EVI1 gene expression in human acute myelogenous leukemias by translocations spanning 300–400 kilobases on chromosome band 3q26. *Proc Natl Acad Sci USA.* 1992; **89**: 3937–3941.
5 Lugthart S, Gröschel S, Beverloo HB, Kayser S, Valk PJ, van Zelderen-Bhola SL *et al.* Clinical, molecular, and prognostic significance of WHO type inv(3)(q21q26.2)/t(3;3)(q21;q26.2) and various other 3q abnormalities in acute myeloid leukemia. *J Clin Oncol* 2010; **28**: 3890–3898.
6 Barjesteh van Waalwijk van Doorn-Khosrovani S, Erpelinck C, van Putten WL, Valk PJ, van der Poel-van de Luytgaarde S, Hack R *et al.* High EVI1 expression predicts poor survival in acute myeloid leukemia: a study of 319 *de novo* AML patients. *Blood* 2003; **101**: 837–845.
7 Lugthart S, van Drunen E, van Norden Y, van Hoven A, Erpelinck CA, Valk PJ *et al.* High EVI1 levels predict adverse outcome in acute myeloid leukemia: prevalence of EVI1 overexpression and chromosome 3q26 abnormalities underestimated. *Blood* 2008; **111**: 4329–4337.
8 Groschel S, Lugthart S, Schlenk RF, Valk PJ, Eiwen K, Goudswaard C *et al.* High EVI1 expression predicts outcome in younger adult patients with acute myeloid leukemia and is associated with distinct cytogenetic abnormalities. *J Clin Oncol* 2010; **28**: 2101–2107.
9 Valk PJ, Verhaak RG, Beijen MA, Erpelinck CA, Barjesteh van Waalwijk van Doorn-Khosrovani S, Boer JM *et al.* Prognostically useful gene-expression profiles in acute myeloid leukemia. *N Engl J Med* 2004; **350**: 1617–1628.
10 Verhaak RG, Wouters BJ, Erpelinck CA, Abbas S, Beverloo HB, Lugthart S *et al.* Prediction of molecular subtype in acute myeloid leukemia based on gene expression profiling. *Haematologica* 2009; **94**: 131–134.
11 Eppert K, Takenaka K, Lechman ER, Waldron L, Nilsson B, van Galen P *et al.* Stem cell gene expression programs influence clinical outcome in human leukemia. *Nat Med* 2011; **17**: 1086–1093.
12 Yuasa H, Oike Y, Iwama A, Nishikata I, Sugiyama D, Perkins A *et al.* Oncogenic transcription factor Evi1 regulates hematopoietic stem cell proliferation through GATA-2 expression. *EMBO J.* 2005; **24**: 1976–1987.
13 Goyama S, Yamamoto G, Shimabe M, Sato T, Ichikawa M, Ogawa S *et al.* Evi-1 is a critical regulator for hematopoietic stem cells and transformed leukemic cells. *Cell Stem Cell* 2008; **3**: 207–220.
14 Saito Y, Nakahata S, Yamakawa N, Kaneda K, Ichihara E, Suekane A *et al.* CD52 as a molecular target for immunotherapy to treat acute myeloid leukemia with high EVI1 expression. *Leukemia* 2011; **25**: 921–931.
15 Yamakawa N, Kaneda K, Saito Y, Ichihara E, Morishita K. The increased expression of integrin a6 (ITGA6) enhances drug resistance in EVI1high leukemia. *PLoS ONE* 2012; **7**: e30706.
16 Ichihara E, Kaneda K, Saito Y, Yamakawa N, Morishita K. Angiopoietin1 contributes to the maintenance of cell quiescence in EVI1high leukemia cells. *BBRC* 2011; **416**: 239–245.
17 Piao X, Hill RS, Bodell A, Chang BS, Basel-Vanagaite L, Straussberg R *et al.* G protein-coupled receptor-dependent development of human frontal cortex. *Science* 2004; **303**: 2033–2036.
18 Li S, Jin Z, Koirala S, Bu L, Xu L, Hynes RO *et al.* GPR56 regulates pial basement membrane integrity and cortical lamination. *J Neurosci* 2008; **28**: 5817–5826.
19 Koirala S, Jin Z, Piao X, Corfas G. GPR56-regulated granule cell adhesion is essential for rostral cerebellar development. *J Neurosci* 2009; **29**: 7439–7449.
20 Iguchi T, Sakata K, Yoshizaki K, Tago K, Mizuno N, Itoh H. Orphan G protein-coupled receptor GPR56 regulates neural progenitor cell migration via a G alpha 12/13 and Rho pathway. *J Biol Chem* 2008; **283**: 14469–14478.
21 Shashidhar S, Lorente G, Nagavarapu U, Nelson A, Kuo J, Cummins J *et al.* GPR56 is a GPCR that is overexpressed in gliomas and functions in tumor cell adhesion. *Oncogene* 2005; **24**: 1673–1682.
22 Xu L, Begum S, Hearn JD, Hynes RO. GPR56, an atypical G protein-coupled receptor, binds tissue transglutaminase, TG2, and inhibits melanoma tumor growth and metastasis. *Proc Natl Acad Sci USA* 2006; **103**: 9023–9028.
23 Ke N, Sundaram R, Liu G, Chionis J, Fan W, Rogers C *et al.* Orphan G protein-coupled receptor GPR56 plays a role in cell transformation and tumorigenesis involving the cell adhesion pathway. *Mol Cancer Ther* 2007; **6**: 1840–1850.
24 Terskikh AV, Easterday MC, Li L, Hood L, Kornblum HI, Geschwind DH *et al.* From hematopoiesis to neuropoiesis: evidence of overlapping genetic programs. *Proc Natl Acad Sci USA* 2001; **98**: 7934–7939.
25 Yang FC, Atkinson SJ, Gu Y, Borneo JB, Roberts AW, Zheng Y *et al.* Rac and Cdc42 GTPases control hematopoietic stem cell shape, adhesion, migration, and mobilization. *Proc Natl Acad Sci USA* 2001; **98**: 5614–5618.
26 Cancelas JA, Lee AW, Prabhakar R, Stringer KF, Zheng Y, Williams DA. Rac GTPases differentially integrate signals regulating hematopoietic stem cell localization. *Nat Med* 2005; **11**: 886–891.
27 Gu Y, Filippi MD, Cancelas JA, Siefring JE, Williams EP, Jasti AC *et al.* Hematopoietic cell regulation by Rac1 and Rac2 guanosine triphosphatases. *Science* 2003; **302**: 445–449.
28 Ghiaur G, Lee A, Bailey J, Cancelas JA, Zheng Y, Williams DA. Inhibition of RhoA GTPase activity enhances hematopoietic stem and progenitor cell proliferation and engraftment. *Blood* 2006; **108**: 2087–2094.
29 Yang L, Wang L, Geiger H, Cancelas JA, Mo J, Zheng Y. Rho GTPase Cdc42 coordinates hematopoietic stem cell quiescence and niche interaction in the bone marrow. *Proc Natl Acad Sci USA* 2007; **104**: 5091–5096.
30 Ghiaur G, Ferkowicz MJ, Milsom MD, Bailey J, Witte D, Cancelas JA *et al.* Rac1 is essential for intraembryonic hematopoiesis and for the initial seeding of fetal liver with definitive hematopoietic progenitor cells. *Blood* 2008; **111**: 3313–3321.
31 Luo R, Jeong SJ, Jin Z, Strokes N, Li S, Piao X. G protein-coupled receptor 56 and collagen III, a receptor-ligand pair, regulates cortical development and lamination. *Proc Natl Acad Sci USA* 2011; **108**: 12925–12930.
32 Xu H, Eleswarapu S, Geiger H, Szczur K, Daria D, Zheng Y *et al.* Loss of Rho GTPase activating protein p190-B enhances hematopoietic stem cell engraftment potential. *Blood* 2009; **114**: 3557–3566.


Supplementary Information accompanies this paper on the Leukemia website (http://www.nature.com/leu)

© 2013 Macmillan Publishers Limited

Zane et al. Retrovirology 2012, 9:114
http://www.retrovirology.com/content/9/1/114

RETROVIROLOGY

RESEARCH Open Access

# Wip1 and p53 contribute to HTLV-1 Tax-induced tumorigenesis

Linda Zane[1], Junichiro Yasunaga[2], Yu Mitagami[2], Venkat Yedavalli[1], Sai-Wen Tang[1], Chia-Yen Chen[1], Lee Ratner[3], Xiongbin Lu[4] and Kuan-Teh Jeang[1*]

## Abstract

**Background:** Human T-cell Leukemia Virus type 1 (HTLV-1) infects 20 million individuals world-wide and causes Adult T-cell Leukemia/Lymphoma (ATLL), a highly aggressive T-cell cancer. ATLL is refractory to treatment with conventional chemotherapy and fewer than 10% of afflicted individuals survive more than 5 years after diagnosis. HTLV-1 encodes a viral oncoprotein, Tax, that functions in transforming virus-infected T-cells into leukemic cells. All ATLL cases are believed to have reduced p53 activity although only a minority of ATLLs have genetic mutations in their p53 gene. It has been suggested that p53 function is inactivated by the Tax protein.

**Results:** Using genetically altered mice, we report here that Tax expression does not achieve a functional equivalence of p53 inactivation as that seen with genetic mutation of p53 (i.e. a $p53^{-/-}$ genotype). Thus, we find statistically significant differences in tumorigenesis between $Tax^{+}p53^{+/+}$ *versus* $Tax^{+}p53^{-/-}$ mice. We also find a role contributed by the cellular Wip1 phosphatase protein in tumor formation in Tax transgenic mice. Notably, $Tax^{+}Wip1^{-/-}$ mice show statistically significant reduced prevalence of tumorigenesis compared to $Tax^{+}Wip1^{+/+}$ counterparts.

**Conclusions:** Our findings provide new insights into contributions by p53 and Wip1 in the *in vivo* oncogenesis of Tax-induced tumors in mice.

## Background

Human T-cell Leukemia Virus type 1 (HTLV-1) is the first identified human retrovirus. The virus belongs to the deltaretrovirus family and is the etiological agent of a highly aggressive neoplastic disease, Adult T-cell Leukemia/Lymphoma (ATLL), and inflammatory diseases including HTLV-1 Associated Myelopathy (HAM)/Tropical Spastic Paraparesis (TSP), uveitis, infective dermatitis and myositis [1-9]. HTLV-1 infects approximately 20 million individuals world-wide, and 1-5% of infected individuals will develop ATLL after a long latency period of 20 to 60 years [1].

HTLV-1 encodes a viral Tax oncoprotein. The singular expression of Tax is sufficient to transform primary rodent cells [10] and potentially human embryonic stem cells [11], immortalize human primary T lymphocytes [12,13], and induce tumors in transgenic mice [14-17]. Tax confers pro-proliferative and pro-survival properties to HTLV-1 infected cells [18-20] by pleiotropically activating effector proteins including the Cyclic AMP Responsive Binding Protein (CREB) and CBP/p300 [21-24], Nuclear Factor kappa-B (NF-κB) [25-29], Cyclin-Dependant Kinases (CDKs) [30-33], and Akt [34-36] amongst others. Tax also triggers DNA damage [37-42]. In transforming a normal T-cell into a leukemic cell, it is believed that Tax must also neutralize cellular checkpoints (e.g. p53 and mitotic spindle assembly checkpoint) that act to censor DNA damage [43,44] and aneuploidy [45,46].

p53 is a DNA-binding transcription factor that plays a key role in cell cycle regulation, apoptosis, and DNA repair [47]. The p53 gene is recognized as one of the most important tumor suppressor genes and is frequently mutated in human tumors including hematologic malignancies [48-50]. In many human malignancies, the frequency of p53 genetic mutation is ≥50% [51,52]; however, the frequency of mutated p53 in ATL patients is reported to be around 15% [53-58], suggesting that loss of p53 activity in ATL may largely arise through a

* Correspondence: KJEANG@nih.gov
[1]Molecular Virology Section, Laboratory of Molecular Microbiology, the National Institutes of Allergy and Infectious Diseases, the National Institutes of Health, Bethesda, Maryland 20892-0460, USA
Full list of author information is available at the end of the article

BioMed Central

© 2012 Zane et al.; licensee BioMed Central Ltd. This is an Open Access article distributed under the terms of the Creative Commons Attribution License (http://creativecommons.org/licenses/by/2.0), which permits unrestricted use, distribution, and reproduction in any medium, provided the original work is properly cited.

mechanism other than genetic mutation. Several *in vitro* studies in different cell types have shown that Tax represses p53 activity [59-65]. Various mechanisms have been proposed for Tax-inactivation of p53. Indeed, it has been suggested that Tax inactivates p53 by acting through either the CREB [62] or the NF-κB [66,67] pathway; however, it has also been noted that neither mechanism satisfactorily explains Tax-p53 interaction [65], leaving the question of how Tax effectively disables p53 function incompletely answered.

Here, we have conducted *in vivo* experiments in mice to address two questions. First, we have assessed the effectiveness of Tax mediated inactivation of p53 *versus* inactivation of p53 by genetic mutations. Second, we have characterized Wip1 as a cooperating *in vivo* Tax co-factor in p53 inactivation. Using various genetically altered mice, we show that Tax inactivation of p53 is functionally less stringent than p53 inactivation by genetic mutation, and we report that the cellular Wip1 phosphatase protein collaborates functionally with Tax in inhibiting p53 activity.

## Results

### $Tax^{+}p53^{-/-}$ mice show reduced tumor free survival compared to $Tax^{+}p53^{+/+}$

In ATLs, p53 genetic mutations are less frequent than those seen in many other cancers [53,54,58]. It has been reasoned that the ability of Tax to inacti-vate p53 function [55] explains why ATL cells may not need to inactivate p53 by genetic mutation. Nevertheless, it has not been clearly characterized whether Tax inactivation of p53 is quantitatively equivalent to inactivation of p53 by genetic mutation. We sought to investigate this issue using gene-tically altered mice. Accordingly, we crossed Tax transgenic mice [15] with $p53^{-/-}$ mutant mice [68] to generate $Tax^{+}p53^{-/-}$, $Tax^{+}p53^{+/-}$ and $Tax^{+}p53^{+/+}$ progenies. We analyzed the genotypes (Figure 1) of the offsprings and monitored the animals over >300 days for tumor development (Figure 2). Tumor-free survival for $Tax^{+}p53^{-/-}$ mice (Figure 2A) was significantly worse compared to $Tax^{+}p53^{+/-}$ and $Tax^{+}p53^{+/+}$ counterparts ($p < 0.0001$; Gehan-Breslow-Wilcoxon test). There were no statistically significant differences in the levels of Tax expression between these two categories of $Tax^{+}$ mice supporting that the difference in tumor-free survival was not due to levels of Tax expression (Additional file 1: Figure S1). Interestingly, no significant difference in tumor-free survival between $Tax^{+}p53^{+/-}$ and $Tax^{+}p53^{+/+}$ mice was found ($p = 0.7093$; Gehan-Breslow-Wilcoxon test); this finding agrees with our previous tumorigenesis study of $p53^{+/-}$ and $p53^{+/+}$ mice [69] that, in the context of our mice, we find no significant functional difference between homozygosity *versus* heterozygosity in wild type p53. Thus, our finding of a distinct difference in tumor-free survival of $Tax^{+}p53^{-/-}$ compared to $Tax^{+}p53^{+/+}$ mice indicates that Tax inactivation of p53 (i.e. $Tax^{+}p53^{+/+}$) is qualitatively less stringent than genetic inactivation of p53 (i.e. $Tax^{+}p53^{-/-}$).

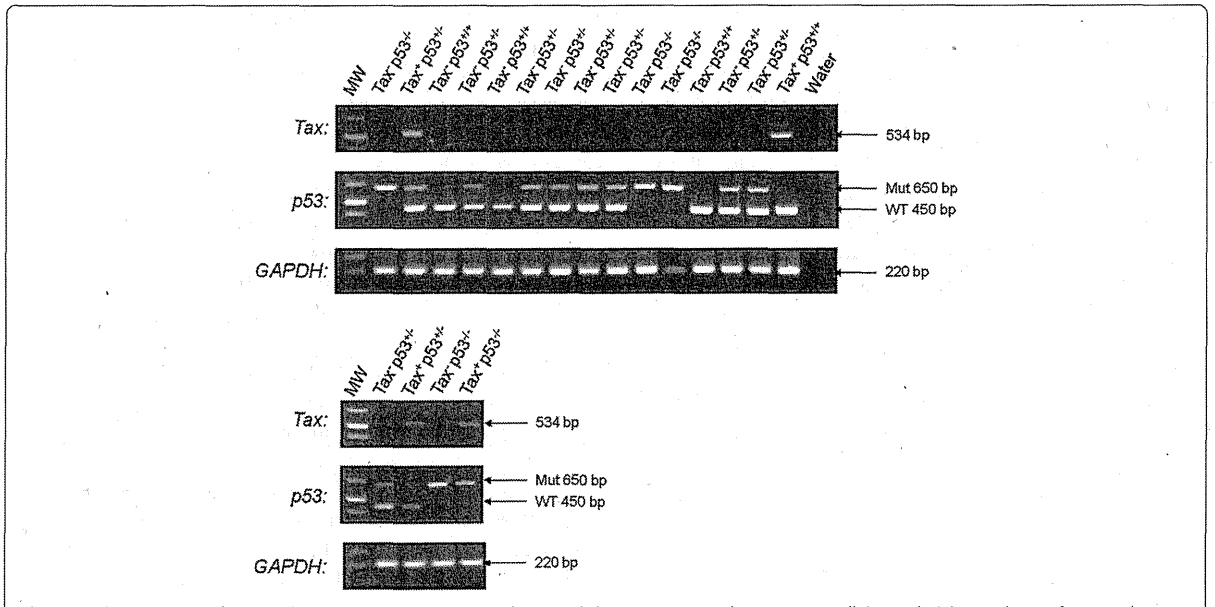


**Figure 1 Genotyping of *p53KO/Tax Tg* mice.** *p53* primers distinguish between WT and mutant p53 alleles with PCR products of 450 and 650 bp in size (top), respectively. Middle panel shows the detection of Tax DNA (534 bp), and the bottom panel shows PCR control detecting cell endogenous GAPDH gene (220 bp). Mut, mutant ; WT, wild type. Tax, p53, and GAPDH signals are as indicated.

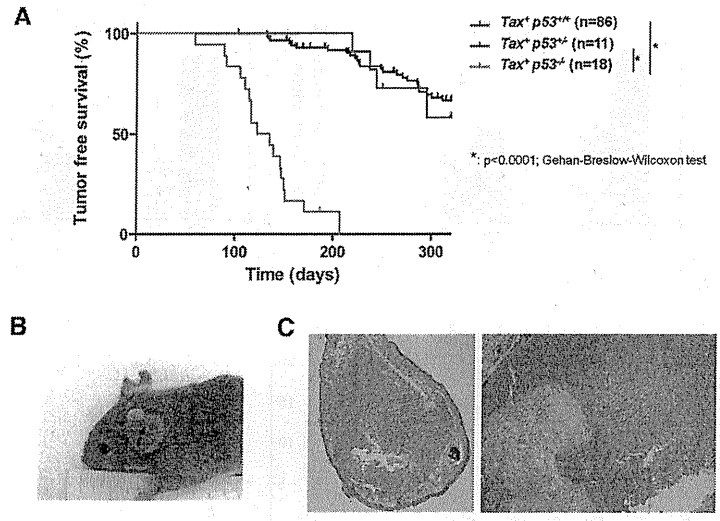


**Figure 2 Statistically significant reduction of tumor-free survival in $Tax^+p53^{-/-}$ mice compared to $Tax^+p53^{+/+}$.** (**A**) Tumor-free survival curves show decreased tumor free survival in $Tax^+p53^{-/-}$ mice compared to $Tax^+p53^{+/-}$ or $Tax^+p53^{+/+}$ animals. Statistical significance (*: p<0.0001) between $Tax^+$ $p53^{-/-}$ and either $Tax^+p53^{+/-}$ or $Tax^+p53^{+/+}$ mice was determined using Gehan-Breslow-Wilcoxon test. (**B**) A Tax transgenic mouse with an ear tumor is shown for illustration. (**C**) Examples of tumor histology [hematoxylin and eosin (H&E) staining] from $Tax^+p53^{+/-}$ mice are shown. Example of a pleomorphic ear sarcoma from a $Tax^+p53^{+/+}$ mouse; (left): expansive soft tissue tumor located in peripheral connective tissue of the ear beneath the supportive cartilage; example of a hind leg pleomorphic histiocytic sarcoma and glandular adenocarcinoma with squamous hyperkeratosis from a $Tax^+p53^{+/+}$ mouse (right): the sarcoma consisted primarily of histiocytic tumor cells with dispersed round cells, sparse spindle cells and neutrophilic granulocytes. Similar tumors are also seen in $Tax^+p53^{-/-}$ mice.

### Wip1 phosphatase modulates p53 activity

We wished next to understand how other non-genetic means of inactivating p53 might cooperate with Tax in cellular transformation. Wip1 (Wild-type p53-induced phosphatase 1) is a human protein phosphatase that has been shown to be amplified and over-expressed in multiple human cancers and has been suggested to exhibit oncogenic potential [70]. A plausible mechanistic scenario could be that Wip1 acts to inhibit p53 activity, thereby contributing to tumorigenesis. Through its ability to inhibit p53 tumor suppressor function, Wip1, like Tax, may reduce the selective pressure for *p53*-inactivating mutations during cancer progression [71,72]. To check the effect of Wip1 on p53, we assessed how its over-expression affects p53's transcriptional activity. Accordingly, we transfected human HCT-116 cells with a luciferase reporter plasmid containing 13 copies of a p53 consensus binding site (pG13-Luc; [73]) together with a Wip1 expression plasmid (Figure 3A and B), or we transfected pG13-Luc with a Tax expression plasmid-alone, or we transfected pG13-Luc with both Wip1 and Tax expression plasmids (Figure 3A and B). Under our transfection conditions, both Wip1-alone and Tax-alone with pG13-Luc robustly repressed the expression of the reporter plasmid by more than 40% ($p=1.496 \times 10^{-5}$ for Wip1-alone; $p=7.62\times10^{-5}$ for Tax-alone; t-test) (Figure 3A). Of note, the co-transfection of Wip1 with Tax repressed pG13-Luc expression by an additional 20% and 15% over that achieved with Tax-alone ($p=0.0025$; t-test) or Wip1 alone ($p=0.019$; t-test) (Figure 3A). When the transfections were performed in the presence of co-introduced exogenous p53, we again observed a statistically significant repression of p53 transcriptional activity; here, we saw >60% repre-ssion of pG13-Luc expression after transfection with Wip1-alone ($p=3.27 \times10^{-5}$; t-test) or Tax-alone ($p=2.22 \times10^{-5}$; t-test) (Figure 3B). In the presence of exogenously introduced p53, the co-transfection of Wip1 and Tax repressed pG13-Luc expression by more than 50% over that achieved with Tax-alone ($p=7.43\times10^{-5}$; t-test) or Wip1-alone ($p=1.25\times10^{-4}$ t-test) (Figure 3B). In Figure 3C, the expression of the transfected plasmids used in Figures 3A and 3B was checked by Western blotting. Taken together, these findings support that Wip1 and Tax cooperate in overall p53 inactivation.

Transient over-expression assays generally are imperfect reflections of physiological regulation. To ask in a more physiological manner how endogenous Wip1 expression regulates p53 activity, we independently isolated several primary MEF clones from $Wip1^{-/-}$ knock-out mice [74] and their $Wip1^{+/+}$ wild type siblings (genotyping examples of MEFs are shown in Figure 3D, top). We then compared cell endogenous p53 activity in several independently isolated $Wip1^{-/-}$ MEFs to other independently isolated control $Wip1^{+/+}$ MEFs employing either the pG13-Luc reporter assay (Figure 3D, bottom) or by determining the mRNA expression levels of a known p53-responsive target gene, $p21^{WAF1/CIP1}$ (Figure 3E). Notably,

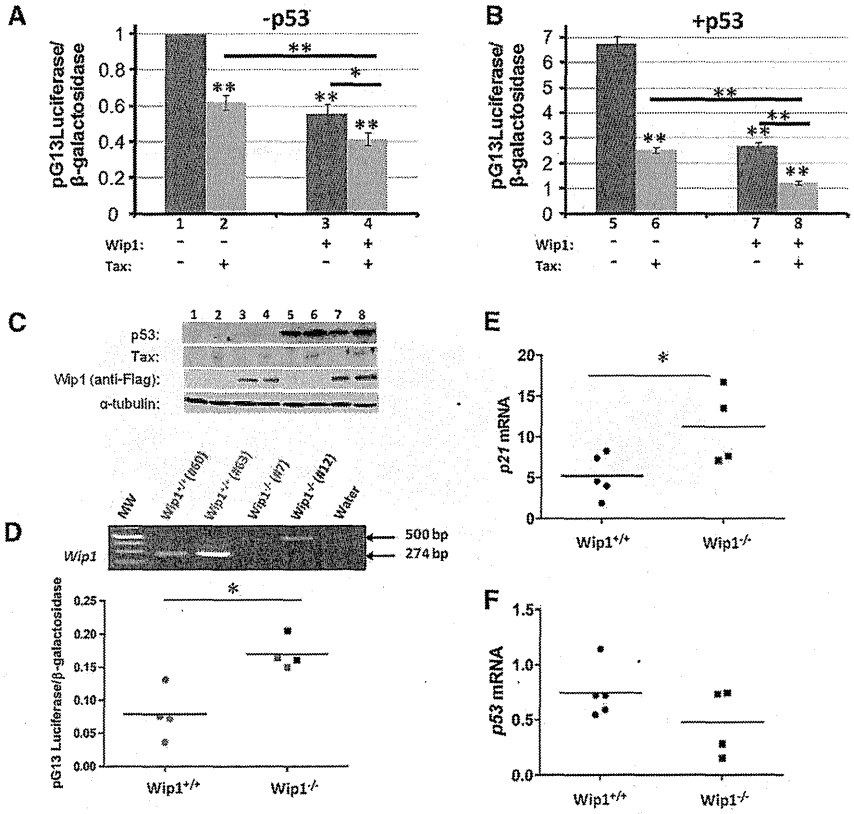


**Figure 3 Wip1 phosphatase attenuates p53 activity.** Wip1 and/or Tax expression reduces p53 transactivation of a pG13Luc-reporter in HCT-116 cells in the absence (**A**) or in the presence (**B**) of exogenous p53 (0.8 μg). HCT-116 cells were transfected with 0.2 μg of Tax and/or 0.75 μg of Wip1 expression plasmid (*: 0.01≤p≤0.05; **: p<0.05; t-test). (**C**) Cell lysates from a representative experiment were subjected to immunoblotting using anti-p53, anti-Tax, anti-Flag and anti-α-tubulin as indicated. The lane numbers of the samples in each case corresponds to the lane numbers indicated in panels (**A**) and (**B**). (**D**) Analysis of cell endogenous p53 activity was conducted using the pG13-Luciferase plasmid in $Wip1^{-/-}$ and $Wip1^{+/+}$ Mouse Embryonic Fibroblasts (MEF). Top panel shows PCR genotypic characterizations of two independent $Wip1^{+/+}$ (60, 63) and two independent $Wip1^{-/-}$ (7, 12) MEFs; each was assayed twice in pG13Luc-reporter assays. Bottom graph shows the luciferase assays. All luciferase activities were normalized to a co-transfected β-galactosidase reporter. Statistical significance was determined using t-test (*: p=0.0076). (**E**) Analyses of cell endogenous p21 and (**F**) p53 mRNAs in 5 independent $Wip1^{+/+}$ (left) and 4 independent $Wip1^{-/-}$ MEFs. Real-time RT-PCR analyses of *p53* and *p21* and *GAPDH* (internal standard) transcripts were performed in $Wip1^{-/-}$ and $Wip1^{+/+}$ MEFs. There was no statistically significant difference in p53 mRNA levels, while p21 mRNA levels were significantly different between $Wip1^{+/+}$ and $Wip1^{-/-}$ MEFs (*: p=0.0425; t-test).

the $Wip1^{-/-}$ MEFs showed statistically significant higher levels of pG13-Luc expression (p=0.0076; t-test) and higher levels of p21 mRNA (p=0.0425; t-test) than the $Wip1^{+/+}$ MEFs, suggesting that cell endogenous Wip1 does physiologically reduce p53 function in primary cells (Figures 3D and E). This regulation of p53 by Wip1, however, does not occur at the level of transcription because there was no statistically significant difference in the amounts of p53 mRNA in $Wip1^{+/+}$ *versus* $Wip1^{-/-}$ MEFs (Figure 3F).

### Wip1 deficiency reduces Tax-tumorigenesis

The above results show that both Wip1 and Tax inactivate p53 function. Next, we asked how the two events might cooperate in tumorigenesis. To address their functional collaboration, we crossed Tax transgenic mice with $Wip1^{+/+}$ or $Wip1^{-/-}$ mice. Various genotypic offsprings were obtained from these crosses (genotyping examples are shown in Figure 4A), and the animals were monitored for tumorigenesis over 300 days (Figure 4B). Interestingly, $Wip1^{+/-}$ and $Wip1^{-/-}$ mice that express Tax showed significantly better tumor-free survival than $Wip1^{+/+}$ animals that express Tax (Figure 4B). Indeed, tumor-free survivals were statistically different between $Tax^{+}Wip^{-/-}$ (p=0.0319; Gehan-Breslow-Wilcoxon test) or $Tax^{+}Wip1^{+/-}$ mice (p=0.0396; Gehan-Breslow-Wilcoxon test) compared to $Tax^{+}Wip1^{+/+}$ mice. In view of findings above that p53 activity is higher in $Wip1^{-/-}$ MEFs

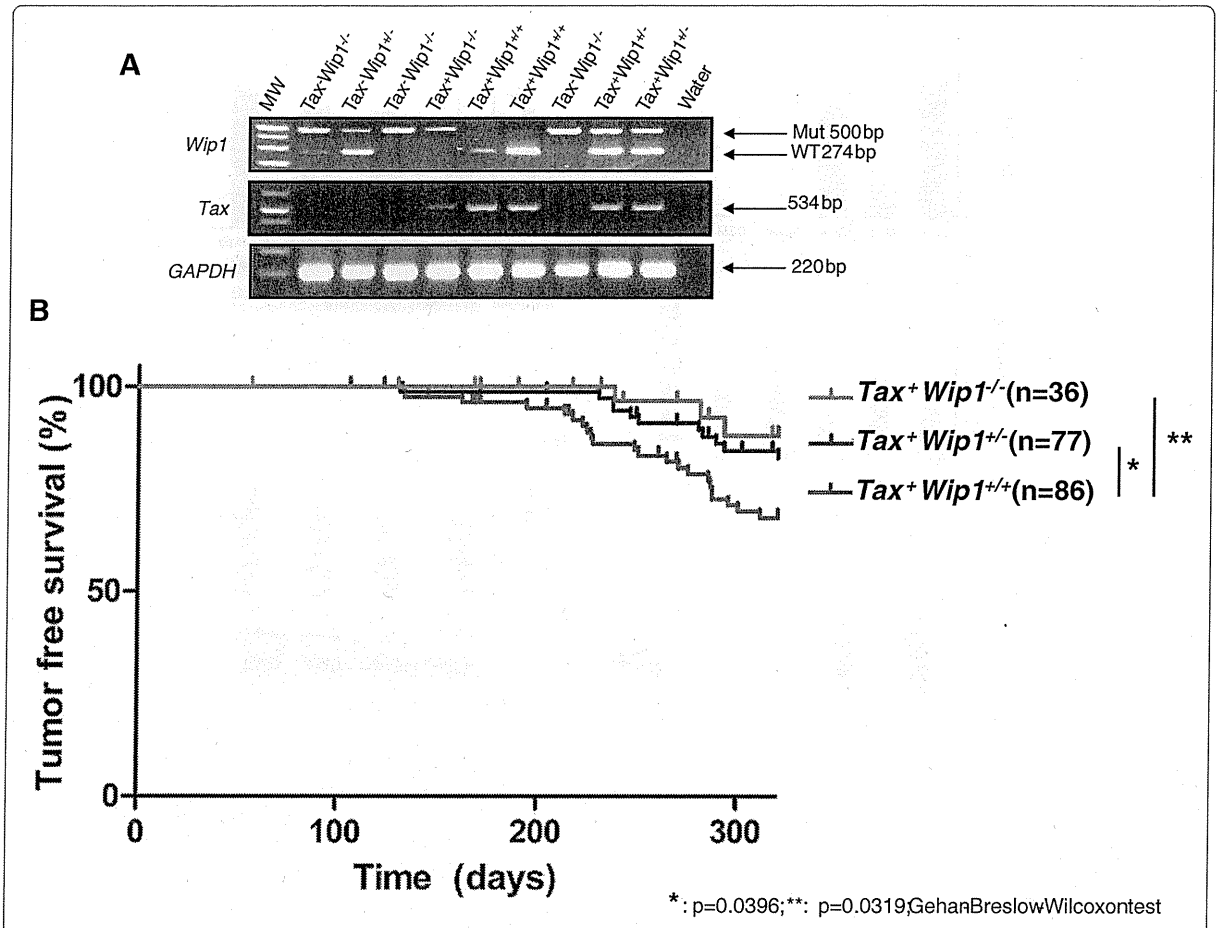


**Figure 4 Statistically significant increase in tumor free survival in $Tax^+Wip1^{-/-}$ mice compared to $Tax^+Wip1^{+/+}$ mice.** (**A**) Genotyping of *Wip1/Tax Tg* mice. The primers for Wip1 distinguish WT and mutant Wip1 alleles with PCR products of 274 and 500 bp, respectively. The GAPDH gene serves as an internal PCR control (220 bp). (**B**) Tumor-free survival curves show increased tumor free survival of $Tax^+$ $Wip1^{-/-}$ and $Tax^+$ $Wip1^{+/-}$ mice compared to $Tax^+$ $Wip1^{+/+}$ animals. Statistically significant (*=p=0.0396 ; **=0.0319) differences between $Tax^+$ $Wip1^{-/-}$ or $Tax^+$ $Wip1^{+/-}$ and $Tax^+$ $Wip1^{+/+}$ mice were determined using Gehan-Breslow-Wilcoxon test.

compared to $Wip1^{+/+}$ MEFs; one interpretation of these *in vivo* tumor results is that homozygous loss of Wip1 (i.e.$Tax^+Wip1^{-/-}$) reduces the level of p53-inactivation in Tax expressing cells compared to counterpart cells that expresses both Wip1 and Tax (i.e. $Tax^+Wip1^{+/+}$); this reduced inactivation of p53 could explain the increased tumor-free survival observed in the $Tax^+Wip1^{-/-}$ over the $Tax^+Wip1^{+/+}$ mice.

### Tax expression does not increase Wip1 transcription

Figure 4B shows that when Tax and Wip1 are expressed together overall *in vivo* transforming potential is increased. Tax is known to activate or repress the transcription of various genes [75-80]; thus a possibility is that Tax expression affects Wip1 transcription. To address this possibility, RNA was isolated from Tax-expressing HTLV-1–transformed MT2, MT4, C8166 cells and compared to RNAs from HTLV-1–negative $CD4^+$ T-cell lines, CEM, Jurkat and H9; specific transcripts were quantified by real-time RT-PCR (Figure 5A). The real-time RT-PCR results showed no correlation between *Tax* expression and *Wip1* expression in these cells. To check in a different way that Tax has no effect on *Wip1* transcription, we transiently transfected p53 $^{-/-}$HCT116 (Figure 5B), $p53^{+/+}$HCT116 (Figure 5C), or HeLa cells (Figure 5D) with various amounts of a Tax expression plasmid and measured Wip1 mRNA. $p53^{-/-}$ HCT116 and $p53^{+/+}$ HCT116 cells [81] have been commonly used to study p53 function. In these cells, we observed no statistically significant change in *Wip1* mRNA upon Tax expression. We also transfected MEFs and HCT-116 cells with a Tax expression plasmid and immunostained the cells for Tax and Wip1 proteins. Based on visualization by confocal microscopy, no difference in

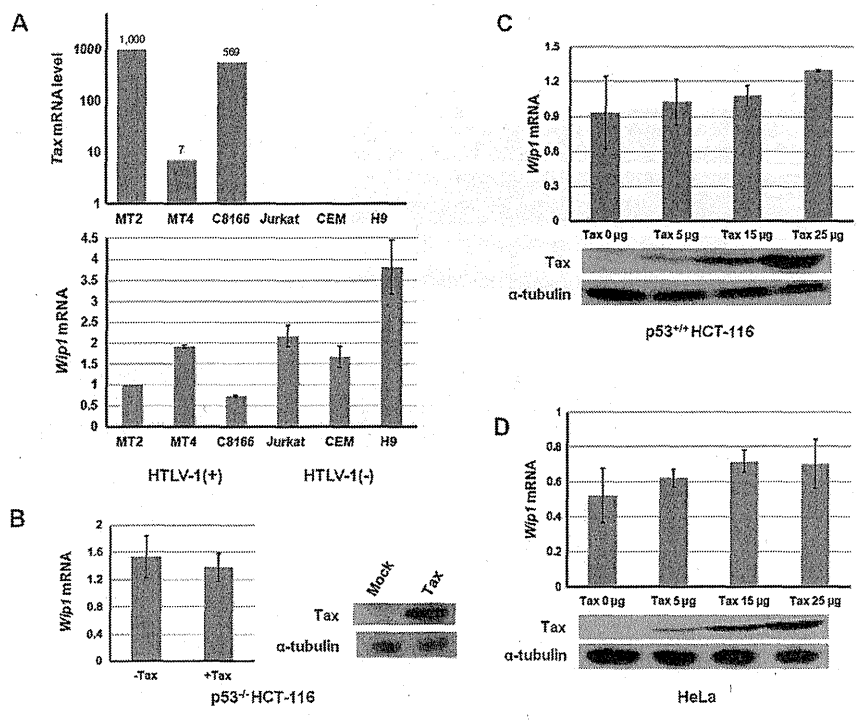


**Figure 5 Analysis of *Wip1* mRNA expression in Tax-expressing and Tax-non-expressing cells.** (**A**) Total RNAs from HTLV-1–transformed MT-2, MT4, C8166 T-cell lines and HTLV-1-negative $CD4^+$ control T-cell lines (Jurkat, CEM, and H9) were extracted and reverse transcribed. The cDNAs were used for real-time RT-PCR analyses of *Wip1*, *Tax*, and *GAPDH* (internal standard) transcripts. The mRNA relative expression levels of *Wip1* and *Tax* mRNA were determined and normalized as multiples of the *GAPDH* mRNA. The columns represent the average results from 3 experiments; the error bars are mean errors. (**B**) Real-time RT-PCR analyses of *Wip1* and *GAPDH* (internal control) transcripts were performed in $p53^{-/-}$ HCT116, (**C**) $p53^{+/+}$ HCT116 and (**D**) HeLa cells after transfection with a control vector or a Tax-expression vector. To detect Tax protein, immunoblots were stained using Tax and α-tubulin specific monoclonal antibodies. Tubulin was used as a loading control.

Wip1 signal intensity was seen in Tax-expressing cells *versus* Tax-negative cells (Figure 6A and Additional file 2: Figure S2A). These findings demonstrate that Tax expression does not change ambient Wip1 protein level and agree with the RNA measurement results that Tax expression does not alter Wip1 mRNA expression (Figure 5).

In our immunostainings, we did note that Tax and Wip1 colocalize in the nucleus (Figure 6A and Additional file 2: Figure S2A). Moreover, additional immunostainings also show that Wip1 and p53 colocalize in the nucleus (Figure 6B and Additional file 2: Figure S2B). Thus, conceivably, Tax, p53, and Wip1 interaction occurs through intranuclear contacts. Currently, we do not have sufficient data to fully understand whether the colocalization of Tax, Wip1, and p53 manifests in direct protein-protein interactions or the proteins interact through bridging by additional factors. Experiments are in progress to define better these mechanistic interactions.

## Discussion

Colloquially known as the guardian of the genome, p53 is an important player in cancer biology, as exemplified by its ubiquitous loss of function in cancers. Thus, approximately 50% of human cancers are genetically mutated in p53 [29,82-85], and the other 50% show attenuated or abrogated p53 activity through means other than mutation [86]. In the case of ATLL, the frequency of p53 gene deletion and mutation is lower than in many other types of cancers and has been reported to approximate 15% [54]. Indeed, our own anecdotal findings are consistent with this low prevalence; in a recent survey of 7 primary ATLL cells, we found no evidence for any of the 11 most frequent p53 somatic gene mutations that have been described for lymphoid neoplasms (Zane, data not shown).

Cancers that retain wild-type p53 gene, nevertheless, can have attenuated p53 activity *via* other mechanisms. For example, Mdm2, an E3 ubiquitin ligase that promotes p53 degradation, is a major negative regulator of p53 [87-89]. Another example of negative regulation arises from the Twist1 protein. Twist1 accumulates in sarcomas that are genotypically p53 wild-type; it dysregulates p53 phosphorylation promoting its degradation [90]. Additional examples come from DNA tumor

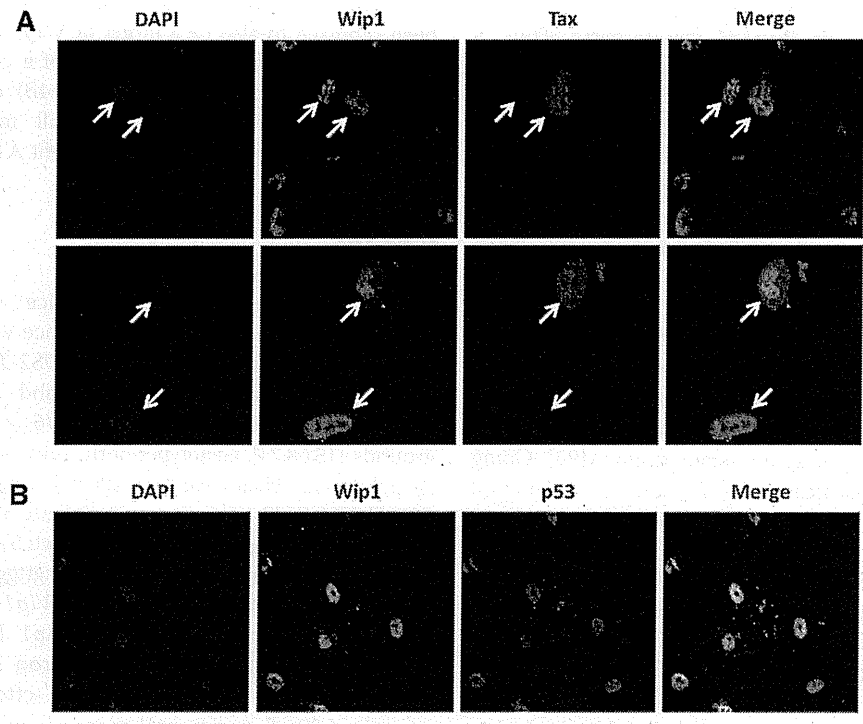


**Figure 6 Confocal analyses of p53, Wip1 and Tax in MEF cells.** (**A**) Analysis of cell endogenous Wip1 and Tax expression and localization by immunofluorescence staining in MEF cells transfected with a Tax expression plasmid for 48 hours. Cells were stained with anti-Tax (red) and anti-Wip1 (green) antibodies. The nuclei were stained with DAPI (blue). Arrows point to cell that expresses Tax (red) and a neighboring cell that does not express Tax. The same two cells are shown to express equal intensities of Wip1 (green). DAPI (blue) stains cellular nuclei. (**B**) The colocalization of cell endogenous p53 and Wip1 in MEF cells. Cells were stained with anti-p53 (red) or anti-Wip1 (green) antibodies, and DAPI was used to stain nuclei (blue).

viruses; some encode proteins that repress p53 activity. Hence, SV40 large T-antigen stabilizes, but inactivates, p53; adenovirus E1B-55-kDa protein, and the E6 oncoprotein of human papilloma virus (HPV) types 16 and 18 target p53 for ubiquitinylation and degradation [91-93]. In the case of HTLV-1, our work here reaffirms previous findings that Tax indeed attenuates p53's transcriptional activity in cultured cells (Figure 3). However, a perhaps more important implication to arise from our study is that we compare for the first time the impact of Tax inactivation of p53 *versus* p53 inactivation by genetic mutation for their relative contributions to *in vivo* tumorigenesis in mice. To date, it generally has been believed that Tax stringently inactivates p53 activity reducing the need for ATL cells to acquire *p53* inactivating mutations. Our results are, however, incongruent with this notion. Thus, we found that Tax induces tumorigenesis in mice much more robustly in a $p53^{-/-}$ setting than in a $p53^{+/+}$ context (Figure 2A), suggesting that Tax inhibition of p53 in the latter context is significantly less complete than p53 inactivation *via* gene mutation. Our findings differ somewhat from those reported by Portis *et al.* [94]. The differences may be due to variances in the mouse numbers, the mouse strains, and the criteria used to determine tumor-free survival and when euthanasias of mice are performed. To date, in the published literature, only cross-sectional findings are associated between p53 genetic mutations and human ATLLs [54]. These findings do not offer clarity on when p53 mutations occurred relative to HTLV-1 infection, Tax expression, and the onset of transformation of ATLL cells. Our results in mice provide prospective analyses of the contribution of a $p53^{-/-}$ genotype to the initiation of *in vivo* tumorigenesis by Tax. Accordingly, extrapolating our mouse findings to humans suggests that early loss of p53 through a $p53^{-/-}$ genetic mutation in cells infected by HTLV-1 foretells a worse prognosis compared to a corresponding infection in a counterpart $p53^{+/+}$ setting.

In our investigation of p53 inactivation, we report for the first time a contributory role by Wip1 in Tax-tumorigenesis. Our insight into the role of Wip1 arose from the observation that loss of Wip1 (i.e. $Wip1^{-/-}$) significantly reduced the frequency of tumor development in Tax transgenic mice (Figure 4B). We linked this observation to a Wip1-mediated p53 effect because we

found that $Wip1^{-/-}$ MEFs have significantly increased p53 activity over their $Wip1^{+/+}$ counterparts. Thus, a parsimonious interpretation of the collective findings is that loss of Wip1 phosphatase (i.e. $Wip1^{-/-}$) increases cell endogenous p53 activity (Figures 3D and E), and this increase in p53 function reduces Tax-tumorigenicity in $Tax^{+}Wip1^{-/-}$ mice (Figure 4B). Hence, the magnitude of p53 activity is important in regulating the extent of *in vivo* Tax tumorigenesis, and this view is further consistent with the tumor-free survival results comparing $Tax^{+}p53^{+/+}$ and $Tax^{+}p53^{-/-}$ mice (Figure 1).

The potential value of inhibiting Wip1 in moderating cancer progression is not only limited to Tax–induced tumors because a Wip1 effect has also been suggested in mammary gland tumors [95], lymphomas [96], colorectal cancers [97], and other spontaneous tumors [98]. Going forward further clarification is needed to understand whether Wip1's effect on many cancers and its impact on Tax-driven tumor formation are primarily due to its effect on p53 signaling or may also arise from its known effects on other pathways, such as ARF, ATM, and p38 MAPK signaling [96,99]. Studies that compare the *in vivo* tumorigenesis frequencies seen in $Tax^{+}Wip1^{-/-}p53^{-/-}$ versus $Tax^{+}Wip1^{+/+}p53^{-/-}$ mice (two genotypes currently being bred in our laboratory) may help to address whether Wip1 has important substrates other than p53 that contribute to Tax-mediated transformation. In other models of carcinogenesis, it has been shown that the singular over-expression of Wip1 is insufficient to initiate oncogenesis [100] and that Wip1 mostly promotes tumors by cooperating with known oncogenes [100]. Nevertheless, amplification of the *Wip1* gene has been described for numerous human primary tumors [101-112], with virtually all such tumors being genetically p53 wild-type [71,72,113]. Based on this observation, one wonders if the low selective pressure for p53 mutations in ATLL could be due to *Wip1* gene amplification in these cells. To our knowledge, this important question has not yet been investigated in ATLLs.

## Conclusions

In summary, despite much progress in HTLV-1 research over the past three decades [114], a salient finding to emerge from this work is the new identification of Wip1 as a cooperating cellular co-factor of Tax in p53-inactivation and *in vivo* tumorigenesis. Currently, our confocal imaging results suggest a colocalization between Tax, Wip1, and p53 within the nucleus (Figure 6 and Additional file 2: Figure S2), but we still lack sufficient data to decipher mechanistically how Tax and Wip1 cooperate to inactivate p53. Amongst several plausible mechanisms, we remain unable to conclude whether Tax can increase Wip1 dephosphorylation of p53 and/or MDM2, a major inhibitor of p53 that has been reported to also be a target of Wip1 [99]. Nonetheless, the functional delineation here of a contribution by Wip1 to Tax tumorigenesis (Figure 4B) does raise the possibility that future uses of small molecule Wip1 phosphatase-inhibitors [115] may benefit ATLL treatment.

## Methods

### Animals and genotyping

The *Tax* and *Wip1*+/– transgenic mice were previously described [15,74]. The *p53*-mutant mice were purchased from the Jackson lab (strain:B6.129S2-*Trp53tm1Tyj*/J) [68]. The Wip1 and p53 knockout and *Tax* transgenic mice were all generated in C57BL/6 × 129/sv backgrounds [15,68,74]. Genotypes of the mice were determined by polymerase chain reactions (PCRs) using primers: *Tax* (Tax-F-7511-7530: 5′-tcggctcagctctacagttc-3′; Tax-R-8044-8025: 5′-tgagggttgagtggaacgga-3′), *p53* (wt: 5′-acagcgtggtgg taccttat-3′, mutant: 5′-ctatcaggacatagcgttgg-3′ and common: 5′-tatactcagagccggcct-3′) and *Wip1* (Wip1 Exon4 F: 5′-gtggagctatgatttcttcagtgg-3′; Wip1 Exon4 R: 5′-g atacgacacaagacaaacctcc-3′; Wip1 intron 3: 5′-acaagcttg cagggctgtttgtgg-3′; PGK promoter: 5′-cttcccagcctctgagc ccagaaagc-3′). Experimental research on mice follows NIH approved animal study protocols and guidelines.

### Analyses of pathologies

Mice were necropsied and examined by mouse pathologists. All of the internal organs (spleen, liver, pancreas, kidney, stomach, intestine, lung, heart, brain, lymph node, thyroid gland) were fixed, paraffin embedded, sectioned and stained with H&E for analyses. Tissues that were found to be grossly abnormal at time of necropsy were multiply sectioned and stained by H&E (hematoxylin and eosin) for microscopic histological analyses.

### Cells and reagents

Human cervical cancer cell line HeLa and human colorectal carcinoma cell lines $p53^{+/+}$HCT116 and $p53^{-/-}$HCT116 [81] were cultured in Dulbecco's modified Eagle's medium containing 10% fetal bovine serum (FBS) and antibiotics. Human T cell lines MT2, MT4, C8166, Jurkat, A301, CEM, and H9 were maintained in RPMI 1640 with 10% FBS.

### Antibodies

Mouse monoclonal anti-Tax (NIH AIDS Research and Reference Reagent Program) was used to detect Tax protein in immunoblotting and by confocal microscopy. Anti-Flag monoclonal antibody (M2; mouse; Sigma), anti-Wip1 polyclonal antibody (rabbit; Santa Cruz), anti-p53

monoclonal antibody (mouse; Cell Signaling) and anti-tubulin monoclonal antibody (DM1A; mouse; Sigma) were purchased.

### Plasmids and transfections

pG13-Luc, p53 (human wild type) (gifts from B. Vogelstein) and Wip1 (gift from L.A. Donehower) expression plasmids were previously described [73,116,117]. HeLa or $p53^{+/+}$ HCT116 or $p53^{-/-}$HCT116 cells were seeded into twelve-well tissue culture plates for the luciferase assays and into 10 cm-dishes for Tax transfections. Transfections were performed 24 h later, using Lipofectamine and Plus reagent (Invitrogen) as described by the manufacturer. At 24 h after transfection of the reporters, cell lysates were subjected to luciferase assay. Total amounts of DNA to be transfected were adjusted by the addition of empty vectors. To detect luciferase and β-Gal activity, luciferase substrate (Promega) and the Galacto-Star assay system (Applied Biosystems) were used. Relative values of luciferase activity were calculated using β-Gal activity as an internal control for transfection.

### Real-time PCR

For real-time quantitative reverse transcriptase–polymerase chain reaction (qRTPCR), total cellular RNA from samples was isolated using TriZol reagent according to the manufacturer's instructions (Invitrogen Life technologies). Before reverse transcription, RNA was treated by DNase (Invitrogen) to prevent DNA contamination. First-strand cDNA was synthesized from 1 μg RNA using oligodT and Superscript III reverse transcriptase (Invitrogen). RNA concentration and purity were determined by UV spectrophotometry (nanodrop). The primer pairs were designed using the Universal Probe Library website (Roche diagnostics) (Wip1-L hs: 5′-cccatgttctacaccaccagt-3′; Wip1-R hs: 5′-tggtccttagaatt caccttg-3′; p53-L hs: 5′-ccccagccaaagaagaaac-3′; p53-R hs: 5′-aacatctcgaagcgctcac-3′; p21-L hs: 5′-cgaagtcagttcct tgtggag-3′; p21-R hs: 5′-catgggttctgacggacat-3′). The primers of each pair were located in different exons to avoid genomic amplification. Primer and probe sequences to detect Tax in human T-cells [118] and Tax-SK43: 5′-cggata cccagtctacgtgt-3′ and Tax-SK44: 5′-gagccgataacgcgtccatcg-3′ to detect Tax in mouse spleens. GAPDH was used as the reference gene for he normalization of results (GAPDH-R: 5′-agtgggtgtcgctgttgaag-3′; GAPDH-F: 5′- tgg tatcgtggaaggactca-3′). PCRs were performed using iQSupermix (Bio-Rad) (for quantification of Tax cDNAs in human T-cells) and iQSYBR Green Supermix (for quantification of other cDNAs) on a CFX96 system (Bio-Rad). A large amount of cDNA was prepared from the MT2, C8166, and MT4 cell lines prior to the experiment. This cDNA was 10 fold-diluted, aliquoted and used as a calibrator for Tax and other RT-PCR runs, respectively. For relative quantification and normalization, the comparative Ct (or Eff-DDC) method was used [119].

### Immunofluorescence

Cells were cultured on glass coverslips, and fixed in 4% paraformaldehyde at 24 h after transfection. After blocking of nonspecific reactions with 1% bovine serum albumin (BSA), cells were then incubated with the indicated primary antibodies, followed by a subsequent incubation with the secondary antibodies conjugated with Alexa Fluor 488 or 594 (Molecular Probes). DNA was counterstained with 0.1 μg/ml Hoechst 33342. Coverslips were mounted in Prolong Antifade (Molecular Probes), and cells were visualized with a Leica TCS SP2 confocal microscope.

### Statistical analyses

The statistical analysis of tumor numbers, survival curves, and spleen weights were computed using the PRISM software (version 5.03).

## Additional files

**Additional file 1: Figure S1.** Analyses of *Tax* mRNA expression in $Tax^{+}$ $p53^{-/-}$ and $Tax^{+}$ $p53^{+/+}$ mouse spleen tissues. Total RNAs from mouse spleen tissues were extracted and reverse transcribed. The cDNAs were used for real-time RT-PCR analyses of Tax and GAPDH (internal standard) transcripts. The mRNA relative expression levels of Tax mRNA were determined and normalized as multiples of the GAPDH mRNA. There was no statistically significant difference in Tax mRNA expression levels between $Tax^{+}$ $p53^{-/-}$ and $Tax^{+}$ $p53^{+/+}$ mice (p=0.2758; unpaired t-test). Each circle or square represents an independent mouse spleen tissue.

**Additional file 2: Figure S2.** Confocal analyses of p53, Wip1 and Tax in MEF cells. (A) Analysis of cell endogenous Wip1 and Tax expression and localization by immunofluorescence staining in HCT-116 cells transfected with a Tax expression plasmid for 48 hours. Cells were stained with anti-Tax (red) and anti-Wip1 (green) antibodies. The nuclei were stained with DAPI (blue). Arrows point to cell that expresses Tax (red) and a neighboring cell that does not express Tax. The same two cells are shown to express equal intensities of Wip1 (green). DAPI (blue) stains cellular nuclei. **(B)** The colocalization of cell endogenous p53 and Wip1 in HCT-116 cells. Cells were stained with anti-p53 (red) or anti-Wip1 (green) antibodies, and DAPI was used to stain the nuclei (blue).

#### Competing interests

*The authors declare that they have no competing interests.*

#### Authors' contributions

LZ designed and performed the work, analyzed the data and wrote the paper. YJ started mouse breedings and genotypings. YM performed some genotypings. VY, SWT and CYC contributed reagents and technical advice for the work and edited the paper. LR and XL provided, respectively, Tax and Wip1 mice and participated in discussions. KTJ conceived of the study and supervised the work and wrote the paper. All authors read and approved the final manuscript.

#### Acknowledgement

*This work was supported by intramural NIAID funding.* XL *was supported by* NIH grant R01CA136549. We thank members of the Jeang laboratory for critical readings of the manuscript; Qingpin Liu for her help with mouse tissues and Melissa Foster and Ryan Hamilton for caring of the mice.

**Author details**
[1]Molecular Virology Section, Laboratory of Molecular Microbiology, the National Institutes of Allergy and Infectious Diseases, the National Institutes of Health, Bethesda, Maryland 20892-0460, USA. [2]Laboratory of Virus Control, Institute for Virus Research, Kyoto University, Kyoto, Japan. [3]Department of Medicine, Washington University School of Medicine, Saint-Louis, Missouri, USA. [4]Department of Cancer Biology, the University of Texas MD Anderson Cancer Center, Houston, Texas, USA.

Received: 16 October 2012 Accepted: 15 December 2012
Published: 21 December 2012

**References**

1. Proietti FA, Carneiro-Proietti AB, Catalan-Soares BC, Murphy EL: **Global epidemiology of HTLV-I infection and associated diseases.** *Oncogene* 2005, 24(39):6058–6068.
2. Poiesz BJ, Ruscetti FW, Gazdar AF, Bunn PA, Minna JD, Gallo RC: **Detection and isolation of type C retrovirus particles from fresh and cultured lymphocytes of a patient with cutaneous T-cell lymphoma.** *Proc Natl Acad Sci U S A* 1980, 77(12):7415–7419.
3. Hinuma Y, Nagata K, Hanaoka M, Nakai M, Matsumoto T, Kinoshita KI, Shirakawa S, Miyoshi I: **Adult T-cell leukemia: antigen in an ATL cell line and detection of antibodies to the antigen in human sera.** *Proc Natl Acad Sci U S A* 1981, 78(10):6476–6480.
4. Miyoshi I, Kubonishi I, Yoshimoto S, Akagi T, Ohtsuki Y, Shiraishi Y, Nagata K, Hinuma Y: **Type C virus particles in a cord T-cell line derived by co-cultivating normal human cord leukocytes and human leukaemic T cells.** *Nature* 1981, 294(5843):770–771.
5. Yoshida M, Miyoshi I, Hinuma Y: **Isolation and characterization of retrovirus from cell lines of human adult T-cell leukemia and its implication in the disease.** *Proc Natl Acad Sci U S A* 1982, 79(6):2031–2035.
6. Watanabe T, Seiki M, Yoshida M: **Retrovirus terminology.** *Science* 1983, 222(4629):1178.
7. Gallo RC: **History of the discoveries of the first human retroviruses: HTLV-1 and HTLV-2.** *Oncogene* 2005, 24(39):5926–5930.
8. Goncalves DU, Proietti FA, Barbosa-Stancioli EF, Martins ML, Ribas JG, Martins-Filho OA, Teixeira-Carvalho A, Peruhype-Magalhaes V, Carneiro-Proietti AB: **HTLV-1-associated myelopathy/tropical spastic paraparesis (HAM/TSP) inflammatory network.** *Inflamm Allergy Drug Targets* 2008, 7(2):98–107.
9. Gessain A, Mahieux R: **Tropical spastic paraparesis and HTLV-1 associated myelopathy: clinical, epidemiological, virological and therapeutic aspects.** *Rev Neurol (Paris)* 2012, 168(3):257–269.
10. Tanaka A, Takahashi C, Yamaoka S, Nosaka T, Maki M, Hatanaka M: **Oncogenic transformation by the tax gene of human T-cell leukemia virus type I in vitro.** *Proc Natl Acad Sci U S A* 1990, 87(3):1071–1075.
11. Zane L, Yasunaga J, Kinjo T, de Melo G, Jeang KT: **Transformation of human embryonic stem cells by HTLV-1 Tax.** *Retrovirology* 2011, 8(Suppl 1):A164.
12. Grassmann R, Berchtold S, Radant I, Alt M, Fleckenstein B, Sodroski JG, Haseltine WA, Ramstedt U: **Role of human T-cell leukemia virus type 1 X region proteins in immortalization of primary human lymphocytes in culture.** *J Virol* 1992, 66(7):4570–4575.
13. Rosin O, Koch C, Schmitt I, Semmes OJ, Jeang KT, Grassmann R: **A human T-cell leukemia virus Tax variant incapable of activating NF-kappaB retains its immortalizing potential for primary T-lymphocytes.** *J Biol Chem* 1998, 273(12):6698–6703.
14. Nerenberg M, Hinrichs SH, Reynolds RK, Khoury G, Jay G: **The tat gene of human T-lymphotropic virus type 1 induces mesenchymal tumors in transgenic mice.** *Science* 1987, 237(4820):1324–1329.
15. Grossman WJ, Kimata JT, Wong FH, Zutter M, Ley TJ, Ratner L: **Development of leukemia in mice transgenic for the tax gene of human T-cell leukemia virus type I.** *Proc Natl Acad Sci U S A* 1995, 92(4):1057–1061.
16. Hasegawa H, Sawa H, Lewis MJ, Orba Y, Sheehy N, Yamamoto Y, Ichinohe T, Tsunetsugu-Yokota Y, Katano H, Takahashi H, *et al*: **Thymus-derived leukemia-lymphoma in mice transgenic for the Tax gene of human T-lymphotropic virus type I.** *Nat Med* 2006, 12(4):466–472.
17. Ohsugi T, Kumasaka T, Okada S, Urano T: **The Tax protein of HTLV-1 promotes oncogenesis in not only immature T cells but also mature T cells.** *Nat Med* 2007, 13(5):527–528.
18. Grassmann R, Aboud M, Jeang KT: **Molecular mechanisms of cellular transformation by HTLV-1 Tax.** *Oncogene* 2005, 24(39):5976–5985.
19. Matsuoka M, Jeang KT: **Human T-cell leukemia virus type 1 (HTLV-1) and leukemic transformation: viral infectivity, Tax, HBZ and therapy.** *Oncogene* 2011, 30(12):1379–1389.
20. Zane L, Sibon D, Jeannin L, Zandecki M, Delfau-Larue MH, Gessain A, Gout O, Pinatel C, Lancon A, Mortreux F, *et al*: **Tax gene expression and cell cycling but not cell death are selected during HTLV-1 infection in vivo.** *Retrovirology* 2010, 7:17.
21. Jeang KT, Boros I, Brady J, Radonovich M, Khoury G: **Characterization of cellular factors that interact with the human T-cell leukemia virus type I p40x-responsive 21-base-pair sequence.** *J Virol* 1988, 62(12):4499–4509.
22. Goren I, Semmes OJ, Jeang KT, Moelling K: **The amino terminus of Tax is required for interaction with the cyclic AMP response element binding protein.** *J Virol* 1995, 69(9):5806–5811.
23. Tie F, Adya N, Greene WC, Giam CZ: **Interaction of the human T-lymphotropic virus type 1 Tax dimer with CREB and the viral 21-base-pair repeat.** *J Virol* 1996, 70(12):8368–8374.
24. Harrod R, Tang Y, Nicot C, Lu HS, Vassilev A, Nakatani Y, Giam CZ: **An exposed KID-like domain in human T-cell lymphotropic virus type 1 Tax is responsible for the recruitment of coactivators CBP/p300.** *Mol Cell Biol* 1998, 18(9):5052–5061.
25. Harhaj EW, Sun SC: **IKKgamma serves as a docking subunit of the IkappaB kinase (IKK) and mediates interaction of IKK with the human T-cell leukemia virus Tax protein.** *J Biol Chem* 1999, 274(33):22911–22914.
26. Xiao G, Cvijic ME, Fong A, Harhaj EW, Uhlik MT, Waterfield M, Sun SC: **Retroviral oncoprotein Tax induces processing of NF-kappaB2/p100 in T cells: evidence for the involvement of IKKalpha.** *EMBO J* 2001, 20(23):6805–6815.
27. Iha H, Kibler KV, Yedavalli VR, Peloponese JM, Haller K, Miyazato A, Kasai T, Jeang KT: **Segregation of NF-kappaB activation through NEMO/IKKgamma by Tax and TNFalpha: implications for stimulus-specific interruption of oncogenic signaling.** *Oncogene* 2003, 22(55):8912–8923.
28. Qu Z, Xiao G: **Human T-cell lymphotropic virus: a model of NF-kappaB-associated tumorigenesis.** *Viruses* 2011, 3(6):714–749.
29. Fu DX, Kuo YL, Liu BY, Jeang KT, Giam CZ: **Human T-lymphotropic virus type I tax activates I-kappa B kinase by inhibiting I-kappa B kinase-associated serine/threonine protein phosphatase 2A.** *J Biol Chem* 2003, 278(3):1487–1493.
30. Iwanaga R, Ohtani K, Hayashi T, Nakamura M: **Molecular mechanism of cell cycle progression induced by the oncogene product Tax of human T-cell leukemia virus type I.** *Oncogene* 2001, 20(17):2055–2067.
31. Haller K, Wu Y, Derow E, Schmitt I, Jeang KT, Grassmann R: **Physical interaction of human T-cell leukemia virus type 1 Tax with cyclin-dependent kinase 4 stimulates the phosphorylation of retinoblastoma protein.** *Mol Cell Biol* 2002, 22(10):3327–3338.
32. Fraedrich K, Muller B, Grassmann R: **The HTLV-1 Tax protein binding domain of cyclin-dependent kinase 4 (CDK4) includes the regulatory PSTAIRE helix.** *Retrovirology* 2005, 2:54.
33. Neuveut C, Low KG, Maldarelli F, Schmitt I, Majone F, Grassmann R, Jeang KT: **Human T-cell leukemia virus type 1 Tax and cell cycle progression: role of cyclin D-cdk and p110Rb.** *Mol Cell Biol* 1998, 18(6):3620–3632.
34. Jeong SJ, Dasgupta A, Jung KJ, Um JH, Burke A, Park HU, Brady JN: **PI3K/AKT inhibition induces caspase-dependent apoptosis in HTLV-1-transformed cells.** *Virology* 2008, 370(2):264–272.
35. Liu Y, Wang Y, Yamakuchi M, Masuda S, Tokioka T, Yamaoka S, Maruyama I, Kitajima I: **Phosphoinositide-3 kinase-PKB/Akt pathway activation is involved in fibroblast Rat-1 transformation by human T-cell leukemia virus type I tax.** *Oncogene* 2001, 20(20):2514–2526.
36. Peloponese JM Jr, Jeang KT: **Role for Akt/protein kinase B and activator protein-1 in cellular proliferation induced by the human T-cell leukemia virus type 1 tax oncoprotein.** *J Biol Chem* 2006, 281(13):8927–8938.
37. Majone F, Semmes OJ, Jeang KT: **Induction of micronuclei by HTLV-I Tax: a cellular assay for function.** *Virology* 1993, 193(1):456–459.
38. Semmes OJ, Majone F, Cantemir C, Turchetto L, Hjelle B, Jeang KT: **HTLV-I and HTLV-II Tax: differences in induction of micronuclei in cells and transcriptional activation of viral LTRs.** *Virology* 1996, 217(1):373–379.
39. Kinjo T, Ham-Terhune J, Peloponese JM Jr, Jeang KT: **Induction of reactive oxygen species by human T-cell leukemia virus type 1 tax correlates with DNA damage and expression of cellular senescence marker.** *J Virol* 2010, 84(10):5431–5437.

40. Majone F, Jeang KT: **Unstabilized DNA breaks in HTLV-1 Tax expressing cells correlate with functional targeting of Ku80, not PKcs, XRCC4, or H2AX.** *Cell Biosci* 2012, **2**(1):15.
41. Durkin SS, Guo X, Fryrear KA, Mihaylova VT, Gupta SK, Belgnaoui SM, Haoudi A, Kupfer GM, Semmes OJ: **HTLV-1 Tax oncoprotein subverts the cellular DNA damage response via binding to DNA-dependent protein kinase.** *J Biol Chem* 2008, **283**(52):36311–36320.
42. Gatza ML, Dayaram T, Marriott SJ: **Ubiquitination of HTLV-I Tax in response to DNA damage regulates nuclear complex formation and nuclear export.** *Retrovirology* 2007, **4**:95.
43. Hanahan D, Weinberg RA: **The hallmarks of cancer.** *Cell* 2000, **100**(1):57–70.
44. Hanahan D, Weinberg RA: **Hallmarks of cancer: the next generation.** *Cell* 2011, **144**(5):646–674.
45. Jin DY, Spencer F, Jeang KT: **Human T cell leukemia virus type 1 oncoprotein Tax targets the human mitotic checkpoint protein MAD1.** *Cell* 1998, **93**(1):81–91.
46. Yasunaga J, Jeang KT: **Viral transformation and aneuploidy.** *Environ Mol Mutagen* 2009, **50**(8):733–740.
47. Vousden KH, Lu X: **Live or let die: the cell's response to p53.** *Nat Rev Cancer* 2002, **2**(8):594–604.
48. Zenz T, Benner A, Dohner H, Stilgenbauer S: **Chronic lymphocytic leukemia and treatment resistance in cancer: the role of the p53 pathway.** *Cell Cycle* 2008, **7**(24):3810–3814.
49. Freed-Pastor WA, Prives C: **Mutant p53: one name, many proteins.** *Genes Dev* 2012, **26**(12):1268–1286.
50. Xu-Monette ZY, Medeiros LJ, Li Y, Orlowski RZ, Andreeff M, Bueso-Ramos CE, Greiner TC, McDonnell TJ, Young KH: **Dysfunction of the TP53 tumor suppressor gene in lymphoid malignancies.** *Blood* 2012, **119**(16):3668–3683.
51. Toyooka S, Tsuda T, Gazdar AF: **The TP53 gene, tobacco exposure, and lung cancer.** *Hum Mutat* 2003, **21**(3):229–239.
52. Iacopetta B: **TP53 mutation in colorectal cancer.** *Hum Mutat* 2003, **21**(3):271–276.
53. Hatta Y, Koeffler HP: **Role of tumor suppressor genes in the development of adult T cell leukemia/lymphoma (ATLL).** *Leukemia* 2002, **16**(6):1069–1085.
54. Tawara M, Hogerzeil SJ, Yamada Y, Takasaki Y, Soda H, Hasegawa H, Murata K, Ikeda S, Imaizumi Y, Sugahara K, *et al*: **Impact of p53 aberration on the progression of Adult T-cell Leukemia/Lymphoma.** *Cancer Lett* 2006, **234**(2):249–255.
55. Tabakin-Fix Y, Azran I, Schavinky-Khrapunsky Y, Levy O, Aboud M: **Functional inactivation of p53 by human T-cell leukemia virus type 1 Tax protein: mechanisms and clinical implications.** *Carcinogenesis* 2006, **27**(4):673–681.
56. Nagai H, Kinoshita T, Imamura J, Murakami Y, Hayashi K, Mukai K, Ikeda S, Tobinai K, Saito H, Shimoyama M, *et al*: **Genetic alteration of p53 in some patients with adult T-cell leukemia.** *Jpn J Cancer Res* 1991, **82**(12):1421–1427.
57. Sakashita A, Hattori T, Miller CW, Suzushima H, Asou N, Takatsuki K, Koeffler HP: **Mutations of the p53 gene in adult T-cell leukemia.** *Blood* 1992, **79**(2):477–480.
58. Reid RL, Lindholm PF, Mireskandari A, Dittmer J, Brady JN: **Stabilization of wild-type p53 in human T-lymphocytes transformed by HTLV-I.** *Oncogene* 1993, **8**(11):3029–3036.
59. Pise-Masison CA, Choi KS, Radonovich M, Dittmer J, Kim SJ, Brady JN: **Inhibition of p53 transactivation function by the human T-cell lymphotropic virus type 1 Tax protein.** *J Virol* 1998, **72**(2):1165–1170.
60. Pise-Masison CA, Radonovich M, Sakaguchi K, Appella E, Brady JN: **Phosphorylation of p53: a novel pathway for p53 inactivation in human T-cell lymphotropic virus type 1-transformed cells.** *J Virol* 1998, **72**(8):6348–6355.
61. Akagi T, Ono H, Tsuchida N, Shimotohno K: **Aberrant expression and function of p53 in T-cells immortalized by HTLV-I Tax1.** *FEBS Lett* 1997, **406**(3):263–266.
62. Ariumi Y, Kaida A, Lin JY, Hirota M, Masui O, Yamaoka S, Taya Y, Shimotohno K: **HTLV-1 tax oncoprotein represses the p53-mediated trans-activation function through coactivator CBP sequestration.** *Oncogene* 2000, **19**(12):1491–1499.
63. Pise-Masison CA, Mahieux R, Radonovich M, Jiang H, Brady JN: **Human T-lymphotropic virus type I Tax protein utilizes distinct pathways for p53 inhibition that are cell type-dependent.** *J Biol Chem* 2001, **276**(1):200–205.
64. Van PL, Yim KW, Jin DY, Dapolito G, Kurimasa A, Jeang KT: **Genetic evidence of a role for ATM in functional interaction between human T-cell leukemia virus type 1 Tax and p53.** *J Virol* 2001, **75**(1):396–407.
65. Miyazato A, Sheleg S, Iha H, Li Y, Jeang KT: **Evidence for NF-kappaB- and CBP-independent repression of p53's transcriptional activity by human T-cell leukemia virus type 1 Tax in mouse embryo and primary human fibroblasts.** *J Virol* 2005, **79**(14):9346–9350.
66. Pise-Masison CA, Mahieux R, Jiang H, Ashcroft M, Radonovich M, Duvall J, Guillerm C, Brady JN: **Inactivation of p53 by human T-cell lymphotropic virus type 1 Tax requires activation of the NF-kappaB pathway and is dependent on p53 phosphorylation.** *Mol Cell Biol* 2000, **20**(10):3377–3386.
67. Jeong SJ, Radonovich M, Brady JN, Pise-Masison CA: **HTLV-I Tax induces a novel interaction between p65/RelA and p53 that results in inhibition of p53 transcriptional activity.** *Blood* 2004, **104**(5):1490–1497.
68. Jacks T, Remington L, Williams BO, Schmitt EM, Halachmi S, Bronson RT, Weinberg RA: **Tumor spectrum analysis in p53-mutant mice.** *Curr Biol* 1994, **4**(1):1–7.
69. Chi YH, Ward JM, Cheng LI, Yasunaga J, Jeang KT: **Spindle assembly checkpoint and p53 deficiencies cooperate for tumorigenesis in mice.** *Int J Cancer* 2009, **124**(6):1483–1489.
70. Fiscella M, Zhang H, Fan S, Sakaguchi K, Shen S, Mercer WE, Vande Woude GF, O'Connor PM, Appella E: **Wip1, a novel human protein phosphatase that is induced in response to ionizing radiation in a p53-dependent manner.** *Proc Natl Acad Sci U S A* 1997, **94**(12):6048–6053.
71. Bulavin DV, Demidov ON, Saito S, Kauraniemi P, Phillips C, Amundson SA, Ambrosino C, Sauter G, Nebreda AR, Anderson CW, *et al*: **Amplification of PPM1D in human tumors abrogates p53 tumor-suppressor activity.** *Nat Genet* 2002, **31**(2):210–215.
72. Yu E, Ahn YS, Jang SJ, Kim MJ, Yoon HS, Gong G, Choi J: **Overexpression of the wip1 gene abrogates the p38 MAPK/p53/Wip1 pathway and silences p16 expression in human breast cancers.** *Breast Cancer Res Treat* 2007, **101**(3):269–278.
73. el-Deiry WS, Kern SE, Pietenpol JA, Kinzler KW, Vogelstein B: **Definition of a consensus binding site for p53.** *Nat Genet* 1992, **1**(1):45–49.
74. Choi J, Nannenga B, Demidov ON, Bulavin DV, Cooney A, Brayton C, Zhang Y, Mbawuike IN, Bradley A, Appella E, *et al*: **Mice deficient for the wild-type p53-induced phosphatase gene (Wip1) exhibit defects in reproductive organs, immune function, and cell cycle control.** *Mol Cell Biol* 2002, **22**(4):1094–1105.
75. Waldele K, Silbermann K, Schneider G, Ruckes T, Cullen BR, Grassmann R: **Requirement of the human T-cell leukemia virus (HTLV-1) tax-stimulated HIAP-1 gene for the survival of transformed lymphocytes.** *Blood* 2006, **107**(11):4491–4499.
76. Pichler K, Kattan T, Gentzsch J, Kress AK, Taylor GP, Bangham CR, Grassmann R: **Strong induction of 4-1BB, a growth and survival promoting costimulatory receptor, in HTLV-1-infected cultured and patients' T cells by the viral Tax oncoprotein.** *Blood* 2008, **111**(9):4741–4751.
77. Krueger A, Fas SC, Giaisi M, Bleumink M, Merling A, Stumpf C, Baumann S, Holtkotte D, Bosch V, Krammer PH, *et al*: **HTLV-1 Tax protects against CD95-mediated apoptosis by induction of the cellular FLICE-inhibitory protein (c-FLIP).** *Blood* 2006, **107**(10):3933–3939.
78. Jeang KT, Widen SG, Semmes OJ, Wilson SH: **HTLV-I trans-activator protein, tax, is a trans-repressor of the human beta-polymerase gene.** *Science* 1990, **247**(4946):1082–1084.
79. Zhang J, Yamada O, Kida S, Matsushita Y, Yamaoka S, Chagan-Yasutan H, Hattori T: **Identification of CD44 as a downstream target of noncanonical NF-kappaB pathway activated by human T-cell leukemia virus type 1-encoded Tax protein.** *Virology* 2011, **413**(2):244–252.
80. Zane L, Sibon D, Legras C, Lachuer J, Wierinckx A, Mehlen P, Delfau-Larue MH, Gessain A, Gout O, Pinatel C, *et al*: **Clonal expansion of HTLV-1 positive CD8+ cells relies on cIAP-2 but not on c-FLIP expression.** *Virology* 2010, **407**(2):341–351.
81. Bunz F, Dutriaux A, Lengauer C, Waldman T, Zhou S, Brown JP, Sedivy JM, Kinzler KW, Vogelstein B: **Requirement for p53 and p21 to sustain G2 arrest after DNA damage.** *Science* 1998, **282**(5393):1497–1501.
82. Vogelstein B, Lane D, Levine AJ: **Surfing the p53 network.** *Nature* 2000, **408**(6810):307–310.
83. Petitjean A, Achatz MI, Borresen-Dale AL, Hainaut P, Olivier M: **TP53 mutations in human cancers: functional selection and impact on cancer prognosis and outcomes.** *Oncogene* 2007, **26**(15):2157–2165.

84. Petitjean A, Mathe E, Kato S, Ishioka C, Tavtigian SV, Hainaut P, Olivier M: **Impact of mutant p53 functional properties on TP53 mutation patterns and tumor phenotype: lessons from recent developments in the IARC TP53 database.** *Hum Mutat* 2007, **28**(6):622–629.
85. Levine AJ, Oren M: **The first 30 years of p53: growing ever more complex.** *Nat Rev Cancer* 2009, **9**(10):749–758.
86. Polager S, Ginsberg D: **p53 and E2f: partners in life and death.** *Nat Rev Cancer* 2009, **9**(10):738–748.
87. Poyurovsky MV, Prives C: **Unleashing the power of p53: lessons from mice and men.** *Genes Dev* 2006, **20**(2):125–131.
88. Manfredi JJ: **The Mdm2-p53 relationship evolves: Mdm2 swings both ways as an oncogene and a tumor suppressor.** *Genes Dev* 2010, **24**(15):1580–1589.
89. Marine JC, Lozano G: **Mdm2-mediated ubiquitylation: p53 and beyond.** *Cell Death Differ* 2010, **17**(1):93–102.
90. Piccinin S, Tonin E, Sessa S, Demontis S, Rossi S, Pecciarini L, Zanatta L, Pivetta F, Grizzo A, Sonego M, *et al*: **A "Twist box" Code of p53 Inactivation: Twist box:p53 Interaction Promotes p53 Degradation.** *Cancer Cell* 2012, **22**(3):404–415.
91. Levine AJ: **The common mechanisms of transformation by the small DNA tumor viruses: the inactivation of tumor suppressor gene products: p53.** *Virology* 2009, **384**(2):285–293.
92. Atkin SJ, Griffin BE, Dilworth SM: **Polyoma virus and simian virus 40 as cancer models: history and perspectives.** *Semin Cancer Biol* 2009, **19**(4):211–217.
93. Gao P, Zheng J: **Oncogenic virus-mediated cell fusion: new insights into initiation and progression of oncogenic viruses–related cancers.** *Cancer Lett* 2011, **303**(1):1–8.
94. Portis T, Grossman WJ, Harding JC, Hess JL, Ratner L: **Analysis of p53 inactivation in a human T-cell leukemia virus type 1 Tax transgenic mouse model.** *J Virol* 2001, **75**(5):2185–2193.
95. Bulavin DV, Phillips C, Nannenga B, Timofeev O, Donehower LA, Anderson CW, Appella E, Fornace AJ Jr: **Inactivation of the Wip1 phosphatase inhibits mammary tumorigenesis through p38 MAPK-mediated activation of the p16(Ink4a)-p19(Arf) pathway.** *Nat Genet* 2004, **36**(4):343–350.
96. Shreeram S, Hee WK, Demidov ON, Kek C, Yamaguchi H, Fornace AJ Jr, Anderson CW, Appella E, Bulavin DV: **Regulation of ATM/p53-dependent suppression of myc-induced lymphomas by Wip1 phosphatase.** *J Exp Med* 2006, **203**(13):2793–2799.
97. Demidov ON, Timofeev O, Lwin HN, Kek C, Appella E, Bulavin DV: **Wip1 phosphatase regulates p53-dependent apoptosis of stem cells and tumorigenesis in the mouse intestine.** *Cell Stem Cell* 2007, **1**(2):180–190.
98. Nannenga B, Lu X, Dumble M, Van Maanen M, Nguyen TA, Sutton R, Kumar TR, Donehower LA: **Augmented cancer resistance and DNA damage response phenotypes in PPM1D null mice.** *Mol Carcinog* 2006, **45**(8):594–604.
99. Lu X, Nguyen TA, Moon SH, Darlington Y, Sommer M, Donehower LA: **The type 2C phosphatase Wip1: an oncogenic regulator of tumor suppressor and DNA damage response pathways.** *Cancer Metastasis Rev* 2008, **27**(2):123–135.
100. Demidov ON, Kek C, Shreeram S, Timofeev O, Fornace AJ, Appella E, Bulavin DV: **The role of the MKK6/p38 MAPK pathway in Wip1-dependent regulation of ErbB2-driven mammary gland tumorigenesis.** *Oncogene* 2007, **26**(17):2502–2506.
101. Li J, Yang Y, Peng Y, Austin RJ, van Eyndhoven WG, Nguyen KC, Gabriele T, McCurrach ME, Marks JR, Hoey T, *et al*: **Oncogenic properties of PPM1D located within a breast cancer amplification epicenter at 17q23.** *Nat Genet* 2002, **31**(2):133–134.
102. Sinclair CS, Rowley M, Naderi A, Couch FJ: **The 17q23 amplicon and breast cancer.** *Breast Cancer Res Treat* 2003, **78**(3):313–322.
103. Barlund M, Kuukasjarvi T, Syrjakoski K, Auvinen A, Kallioniemi A: **Frequent amplification and overexpression of CCND1 in male breast cancer.** *Int J Cancer* 2004, **111**(6):968–971.
104. Tan DS, Lambros MB, Rayter S, Natrajan R, Vatcheva R, Gao Q, Marchio C, Geyer FC, Savage K, Parry S, *et al*: **PPM1D is a potential therapeutic target in ovarian clear cell carcinomas.** *Clin Cancer Res* 2009, **15**(7):2269–2280.
105. Natrajan R, Lambros MB, Rodriguez-Pinilla SM, Moreno-Bueno G, Tan DS, Marchio C, Vatcheva R, Rayter S, Mahler-Araujo B, Fulford LG, *et al*: **Tiling path genomic profiling of grade 3 invasive ductal breast cancers.** *Clin Cancer Res* 2009, **15**(8):2711–2722.
106. Saito-Ohara F, Imoto I, Inoue J, Hosoi H, Nakagawara A, Sugimoto T, Inazawa J: **PPM1D is a potential target for 17q gain in neuroblastoma.** *Cancer Res* 2003, **63**(8):1876–1883.
107. Castellino RC, De Bortoli M, Lu X, Moon SH, Nguyen TA, Shepard MA, Rao PH, Donehower LA, Kim JY: **Medulloblastomas overexpress the p53-inactivating oncogene WIP1/PPM1D.** *J Neurooncol* 2008, **86**(3):245–256.
108. Mendrzyk F, Radlwimmer B, Joos S, Kokocinski F, Benner A, Stange DE, Neben K, Fiegler H, Carter NP, Reifenberger G, *et al*: **Genomic and protein expression profiling identifies CDK6 as novel independent prognostic marker in medulloblastoma.** *J Clin Oncol* 2005, **23**(34):8853–8862.
109. Ehrbrecht A, Muller U, Wolter M, Hoischen A, Koch A, Radlwimmer B, Actor B, Mincheva A, Pietsch T, Lichter P, *et al*: **Comprehensive genomic analysis of desmoplastic medulloblastomas: identification of novel amplified genes and separate evaluation of the different histological components.** *J Pathol* 2006, **208**(4):554–563.
110. Hirasawa A, Saito-Ohara F, Inoue J, Aoki D, Susumu N, Yokoyama T, Nozawa S, Inazawa J, Imoto I: **Association of 17q21-q24 gain in ovarian clear cell adenocarcinomas with poor prognosis and identification of PPM1D and APPBP2 as likely amplification targets.** *Clin Cancer Res* 2003, **9**(6):1995–2004.
111. Fuku T, Semba S, Yutori H, Yokozaki H: **Increased wild-type p53-induced phosphatase 1 (Wip1 or PPM1D) expression correlated with downregulation of checkpoint kinase 2 in human gastric carcinoma.** *Pathol Int* 2007, **57**(9):566–571.
112. Loukopoulos P, Shibata T, Katoh H, Kokubu A, Sakamoto M, Yamazaki K, Kosuge T, Kanai Y, Hosoda F, Imoto I, *et al*: **Genome-wide array-based comparative genomic hybridization analysis of pancreatic adenocarcinoma: identification of genetic indicators that predict patient outcome.** *Cancer Sci* 2007, **98**(3):392–400.
113. Rauta J, Alarmo EL, Kauraniemi P, Karhu R, Kuukasjarvi T, Kallioniemi A: **The serine-threonine protein phosphatase PPM1D is frequently activated through amplification in aggressive primary breast tumours.** *Breast Cancer Res Treat* 2006, **95**(3):257–263.
114. Martin F, Bangham CR, Ciminale V, Lairmore MD, Murphy EL, Switzer WM, Mahieux R: **Conference highlights of the 15th International Conference on Human Retrovirology: HTLV and related retroviruses, 4–8 June 2011, Leuven, Gembloux, Belgium.** *Retrovirology* 2011, **8**:86.
115. Hayashi R, Tanoue K, Dureil SR, Chatterjee DK, Jenkins LM, Appella DH, Appella E: **Optimization of a cyclic peptide inhibitor of Ser/Thr phosphatase PPM1D (Wip1).** *Biochemistry* 2011, **50**(21):4537–4549.
116. Kern SE, Pietenpol JA, Thiagalingam S, Seymour A, Kinzler KW, Vogelstein B: **Oncogenic forms of p53 inhibit p53-regulated gene expression.** *Science* 1992, **256**(5058):827–830.
117. Choi J, Appella E, Donehower LA: **The structure and expression of the murine wildtype p53-induced phosphatase 1 (Wip1) gene.** *Genomics* 2000, **64**(3):298–306.
118. Yamano Y, Nagai M, Brennan M, Mora CA, Soldan SS, Tomaru U, Takenouchi N, Izumo S, Osame M, Jacobson S: **Correlation of human T-cell lymphotropic virus type 1 (HTLV-1) mRNA with proviral DNA load, virus-specific CD8(+) T cells, and disease severity in HTLV-1-associated myelopathy (HAM/TSP).** *Blood* 2002, **99**(1):88–94.
119. Livak KJ, Schmittgen TD: **Analysis of relative gene expression data using real-time quantitative PCR and the 2(−Delta Delta C(T)) Method.** *Methods* 2001, **25**(4):402–408.

doi:10.1186/1742-4690-9-114
**Cite this article as:** Zane *et al.*: Wip1 and p53 contribute to HTLV-1 Tax-induced tumorigenesis. *Retrovirology* 2012 9:114.